NOTICE

CERTAIN DATA CONTAINED IN THIS DOCUMENT MAY BE DIFFICULT TO READ IN MICROFICHE PRODUCTS.

CONF-9005145--3

DE91 004420

HIGH RESOLUTION ELECTRON MICROSCOPY OF INTERFACES IN FCC MATERIALS*

KARL L. MERKLE
Materials Science Division
Argonne National Laboratory
Argonne, IL 60439

AUGUST 1990

*Work supported by the U.S. Department of Energy, Basic Energy Sciences, under contract W-31-109-Eng-38.

To be submitted to Ultramicroscopy, to be included in the Proceedings of the "Frontiers of Electron Microscopy in Materials Science" Conference, Oak Brook, IL, May 1990.

Abstract

Modern high-resolution electron microscopy (HREM) instruments, which are capable of a point-to-point resolution of better than 0.2 nm, have allowed atomic-scale observations of a variety of internal interfaces. The application of the HREM technique to fcc model systems for the purpose of addressing a number of interface issues will be examined in this paper. Atomic structure observations for heterophase interfaces of metal/metal and metal/metal-oxide systems as well as HREM studies of grain boundaries in NiO and Au will be discussed with emphasis on generic structural features and the role of the interface plane. Comparisons between observed interface structures and atomistic computer modeling results have shown agreements for some interfaces, as well as certain differences in others. A number of structural features are common to both metal and oxide grain boundaries, as well as certain heterophase boundaries. Of particular importance in close-packed solids appears to be the tendency to preserve, as much as possible, local atomic coordination, giving rise to atomically well-matched regions that alternate along the interface with regions of misfit. It is commonly observed that heterophase interfaces are being preferentially formed on dense-packed planes. Low-index planes are also frequently observed in asymmetric grain boundaries. In addition to the observation of misfit dislocations in heterophase boundaries, misfit-dislocation-like defects have also been found in asymmetric, incommensurate grain boundaries. The tendency for maintaining coherence between dense-packed planes across the interface has resulted in the formation of novel three-dimensional GB structures. HREM observations have brought new insights into the correlations between macroscopic geometry, interfacial energy, and microscopic atomic relaxations.

1. Introduction

Internal interfaces in solids are of great importance because they often determine essential properties of materials. Therefore, the investigation of grain boundaries and heterophase boundaries has spanned many decades of intense research. It has long been recognized that our understanding of interface properties hinges strongly on the availability of information about the atomic-scale nature of the interface. While atomistic computer modeling has been used for some time for certain types of planar interfaces, such as periodic grain boundaries, the validity of such studies has to be tested against experiment. Direct atomic-scale observations of a wide range of homo- and heterophase interfaces have become possible with the recent introduction of modern HREM instruments. As a result of these developments considerable advances of our understanding of solid interfaces have already been accomplished.

A combined approach, utilizing theoretical and experimental atomistic investigations appears most promising for improving our understanding of solid interfaces. We review here briefly interfacial foundations and issues as they relate to the HREM examination of atomic structures and present some of our recent HREM observations on grain boundaries (GBs) in close-packed ceramics and metals as well as heterophase boundaries involving these materials. The great potential of the HREM technique for extracting atomic-scale information about interfaces will be obvious from our discussion of presently available results concerning those GB features that may be of general validity for fcc materials.

2. HREM of Internal Interfaces

Axial illumination HREM allows the direct observation of atomic-scale details of crystalline interfaces, provided certain conditions are met [1, 2]. First, atomic resolution

can be obtained when the interface is viewed edge-on along those (low-index) zone axes, for which, on both sides of the interface, the corresponding interplanar spacings are within the point-to-point resolution of the electron microscope. With modern HREM instruments sufficient resolution along low-index zone axes is presently available for most crystalline materials of interest. Second, thin sections ($\lesssim$10 nm) containing the interface must be prepared. For many materials the preparation of suitable interfacial specimens is a major task, and has developed into a sophisticated art. Third, the material must be sufficiently stable under irradiation with the electron beam.

The interpretation of HREM images in terms of the atomic structure requires the capabilities to assess the influence of instrumental parameters (resolution, defocus,etc.) and specimen related parameters (thickness, tilt, etc.). This can be done by comparisons to computer simulated images. A minimal amount of image interpretation is necessary when the structures have the translational symmetry of the lattice in the direction of the electron beam. In this case, images taken near the optimum defocus can be directly interpreted, and, in a qualitative fashion, positions of atomic columns can be deduced from the images. On the other hand, atomic relaxations near the interface are not necessarily confined to displacements normal to the electron beam. Displacements parallel to the electron beam are, of course, not detected by HREM, while normal displacement components that vary with depth give rise to complex images, that can not be directly interpreted, since atomic columns with the translational symmetry of the lattice are not maintained. Another complication arises when point defects are incorporated at an interface. In this case, as is indicated for example for some ceramic oxides, atomic columns may not be fully occupied near the boundary, leading to subtle image contrast effects that may be difficult to separate from experimental artifacts. In any case, image simulations must be considered an important part of HREM interface studies. Such computer simulations are not only

required for the verification of specific atomic boundary models, but are also necessary to avoid misinterpretations of observed images.

Since for observation along a given zone axis, the HREM technique can at best provide a two-dimensional projection of the atomic structure of an interface, a full, three-dimensional atomic-scale characterization will require observation along an additional direction. This will not always be possible, but has in fact been demonstrated [3 , 4]. However, even the rather qualitative examination of a variety of interfaces, has provided a wealth of information about the atomic structure of homo- and heterophase boundaries. Several examples of such observations will be presented in sections 6 and 7.

3. Interface Issues

There are a great number of problems in interface science, whose understanding requires information about the atomic structure of the interface. Two of the most fundamental issues concern the questions, "Which interfaces have low energy?" , and "What is their structure?". From this perspective, we shall examine some of our HREM results on interfacial structure in fcc systems. In preparation for this, as a first step before examining atomic structures of interfaces, an understanding of the macroscopic and microscopic geometries involved in forming an interface is required. In the following section we shall briefly review the foundations of interface geometry and structure in cubic materials, while available information on interfacial energies and atomic relaxations will be discussed in section 5.

4. Interface Geometry

4.1 Macroscopic Geometry

Two crystalline solids can be brought together to form an interface between two single crystals in an infinite variety of ways. As is well known, five macroscopic degrees of freedom (DOF) have to be specified for defining a grain boundary, while heterophase boundaries require for their description a still greater number of parameters, even when no reaction layer is formed between the two solids. The 5 DOFs for a grain boundary can be specified by a misorientation (axis, 2 DOFs, angle, 1 DOF) and a boundary plane (2 DOFs), see fig. 1a. An alternative way to describe a GB is via the two GB planes forming the interface (4 DOFs), and a twist-angle ψ, between the two planes (1 DOF), see fig. 1b. The former description is convenient when describing a bicrystal of a given misorientation. The different inclinations that the GB plane can assume then define the possible GB facets. On the other hand, the specification of an interface by its interface crystallography in terms of the crystallographic planes that are joined at the interface and their relative rotations normal to the interface plane, is of advantage when considering atomic relaxations and energies of GBs [5].

4.2 Interface Symmetries

The well-known coincident site lattice (CSL) model considers two interpenetrating lattices of the (unrelaxed) ideal crystal at the appropriate misorientation. For certain misorientations a superlattice of coincident sites exists, see fig. 2., and a CSL bicrystal is then typically denoted by its reciprocal volume density of coincident sites Σ. Two aspects of this geometric model should be noted: First, at small misorientations, the regions of good and poor atomic matching between the two lattices can be identified. Second, the CSL for a particular boundary governs the translational symmetry of the GB. CSL

boundaries on rational planes are strictly periodic. In fig.2 the shortest periods belong to the two symmetric tilt GBs (see dark arrows). However, this is not always the case, but more importantly for each bicrystal, there is an infinitely large number of possible asymmetric GBs, i. e. GBs that are bounded by two crystallographically different planes.

It is well known from computer simulations and observations, that the CSL is not preserved in real bicrystals, since a rigid-body translation away from the coincidence position is generally required when the GB structure is relaxed to its minimum energy state [6]. Nevertheless, the translational symmetry along the boundary plane is maintained for both symmetric and asymmetric CSL boundaries. For tilt GBs the translational symmetry *of the lattice* is maintained in the direction of the tilt axis. Such boundaries are well suited for HREM investigations, provided the tilt axis coincides with a low-index direction.

For heterophase boundaries it is generally not possible to construct an exact CSL model, since typically the lattice parameter ratios are irrational. An example is given in figure 3 , which illustrates the cube-on-cube superposition of two fcc lattices whose lattice parameters a_1 and a_2 are not rationally related: $a_1/a_2 \neq n/m$. Nevertheless, regions of poor atomic fit alternate with regions of good fit. For many systems so-called near-coincidence models can be constructed, which are based on a periodic interfacial unit cell which approximates the real interfacial geometry [7, 8].

4.3 Interface Periodicities

The periodicity of an interface is primarily given by its bicrystal geometry. Thus a CSL bicrystal conceptually will always generate a periodic boundary as long as the GB lies on a rational plane. However tilt GBs on irrational planes can be considered one dimensional quasicrystals [9, 10]. Ultimately the physically relevant structural units of an

interface are determined by the atomic relaxations . For example, the planar unit cell of a CSL boundary could be modified by reconstruction.

Since heterophase boundaries are typically incommensurate they can, in contrast to CSL boundaries, not have a periodic structure. However, when misfit localization takes place, such interfaces may be viewed as quasiperiodic. In this instance the quasiperiodicity is a result of the formation of regularly spaced misfit dislocations [11-16]. The heterophase boundary depicted in fig. 3b, for example, is incoherent and there is no periodicity along the interface. However, if misfit localization would occur at this interface, the centers of misfit would be spaced in a quasiperiodic manner, when viewed on an atomic scale.

Quasiperiodicities of this type also play a role in grain boundaries, as will be shown in section 7. If we consider for example the GB formed in fig. 2b) from a rigid lattice model, which derives from the exact Σ=17, (100)(8,15,0) asymmetric GB, with a structural repeat unit that spans almost the whole width of fig. 2, it is clear that this boundary could possibly relax towards a smaller structural unit. In fact, the (100)(120) GB which is incommensurate, may form a much more energetically favorable interface, since it consists of the combination of two low index (high atomic density) planes. Relaxation towards such a boundary may be possible, since its misorientation (θ=26.57°) deviates by only 1.5° from the exact Σ=17 misorientation (θ=28.07°).

5. Interfacial Energy and Atomic Relaxations

A fundamental, but largely unresolved question, concerns the interrelations between macroscopic geometry, interfacial energy, and the atomic structure of interfaces. It is now widely recognized, that geometric models, although important for establishing interface symmetries, and possible matching on an atomic scale, in general have no predictive capability regarding the interfacial energy, although in the past, low Σ boundaries have often been considered special. Sutton and Balluffi [17] have recently examined the existing

experimental evidence for low-energy boundary configurations, with the conclusion that no simple geometric criterion suffices to universally predict low-energy interfaces. Nevertheless there must be strong connections between geometry, energy, structure, and composition of interfaces. It is a most challenging endeavor of experimental and theoretical interface science to explore the physically important parameters and relaxation mechanisms that determine low-energy interfaces. Considerable progress concerning the interrelation between GB energy and their macroscopic and microscopic structure has recently been made by computer simulations of GBs in cubic metals, where much of the 5-dimensional GB phase space has now been explored [18-21]. The recent advances in HREM instrumentation make it presently possible to directly examine interface structures on an atomic level. This has been important for testing theoretical predictions and for revealing unforseen relaxation mechanisms at interfaces.

5.1 The role of the interface plane

The major geometric feature determining the energy of an interface is given by the crystallographic planes that are joined at the boundary. Dense-packed planes often are preferred energetically in hetero- as well as homophase boundaries, including free surfaces.

When the two planes joined at the interface are rotated around an axis parallel to the plane normal (see fig. 1b), two positions (that can be characterized by the twist angles ψ=0 and ψ=180°) exist in general for which pure tilt GBs are produced, while all others are either pure twist (for symmetric planes), or general GBs that contain twist, as well as tilt components (asymmetric planes). Recent computer simulations have shown that the pure tilt configurations (at ψ=0° and ψ=180°) always are associated with energy cusps [21]. This result emphasizes the importance of tilt GBs, which fortunately are also the ones accessible to atomic scale experimental investigations via HREM. Therefore, we expect that results obtained from HREM studies of tilt GBs are of general significance for

polycrystalline materials and will advance, together with computer simulations, our understanding of GBs in general.

For heterophase boundaries, the chemical nature of the components and their interactions are of prime importance for determining interface properties. In contrast to metallic interfaces, the bonding across the interface in metal/ceramic interfaces is rather poorly understood, and few theoretical treatments have been attempted [22-24]. Atomic-scale observations in these systems are useful for determining low-energy interfaces, local relaxations, and the type of atoms joined at the interface.

To determine the planar nature of the interface and to unequivocally identify the interface plane, atomic-scale observations (by HREM) are necessary, since macroscopic geometry may not reveal the underlying atomic-scale facets in a given boundary.

5.2 Atomic relaxations in interfaces

Close-packed materials have often been modeled by the packing of hard spheres. Many of the important aspects of these structures can be understood in this manner, and the minimization of the free volume in such structures has in fact been invoked for deriving possible GB structures in fcc systems in terms of polyhedral structural units [25]. However, it is clear, that the details of the interatomic interactions are important in determining the structure that will evolve from a rigid geometric arrangement of atoms when such an assembly is allowed to fully relax to minimize its energy. As mentioned above, considerable progress has been made in recent years, by computer simulating, GBs in particular, based largely on calculations employing two-body and potentials of the embedded atom type [26-30].

For GBs, an important experimental task is to validate the proposed models or results from computer calculations. In addition, unexpected types of relaxations may exist that are accessible to observation by high-resolution techniques. Furthermore, structural detail, such as faceting and steps at interfaces, and interactions with dislocations, are important for understanding GB properties.

In heterophase boundaries, the degree of misfit localization and the form which the misfit defects take can be investigated by HREM. In contrast to tilt GBs, a considerable difficulty derives from the fact that the misfit is three-dimensional and therefore the relaxations at the interface generally destroy the translational symmetry of the lattice in the direction of the electron beam. Consequently, structure comparisons based on theoretical models and image simulations are quite important for heterophase boundaries. Unfortunately, theoretical treatments of relaxations at heterophase boundaries are at this point readily available only for metallic systems.

6. HREM of Heterophase Boundaries

HREM observations allow the determination of a number of parameters of interest for the characterization and properties of heterophase interfaces: 1) identification of preferred interface planes , i. e. which interfaces have low energy; 2) characterization of steps or facets; 3) observation of interface roughness; 4) the identification of the type of atoms that are bonded across the interface 5) the degree of coherency, i. e. whether or not, the misfit is localized in the form of misfit dislocations; 6) the structure of misfit dislocations and elastic relaxations at the boundary ; 7) the periodicity along the interface; and 8) the presence of intrinsic and extrinsic defects such as vacancies, impurity complexes, or second phases at the interface.

Atomic-scale observations of interfaces in semiconductor materials [31] and precipitate interfaces [32] have in the past found considerable attention. Recently a number of metal/ceramic interfaces have also been studied by HREM, for example, Nb/Al_2O_3, Cu/Al_2O_3, Pt/NiO, Cu/NiO, PdNiO, AgCdO, AgNiO etc [33]. The interfaces can be formed by a variety of methods, including epitaxy, pressure-bonding, and as precipitate boundaries. Internal reduction [34] as well as internal oxidation [35] has been used as a convenient means to produce metal/ceramic boundaries that can be studied by HREM.

For fcc systems, the cube-on-cube orientation between precipitate and matrix or between substrate and overlayer is found in most instances. Fundamental issues then concern the possible localization of misfit at the interface, its dependence on geometric parameters and bonding type, as well as interfacial defects and impurities. Very little is known in most of these areas. It is well recognized that misfit dislocations often exist at the interface in heterophase systems of small lattice parameter difference [11, 36]. However, for large misfits, it is generally not known, whether or not, and to what degree misfit localization occurs.

6.1 The Interface Plane

The misfit η is given by $\eta=2(a_1-a_2)/(a_1+a_2)$, where a_1 and a_2 are the lattice parameters of the matrix or substrate and the precipitate or overlayer respectively. Table 1 gives the misfit for several fcc metal/metal and metal/metal-oxide systems that have recently been investigated in our laboratory. The interfaces were produced by internal reduction [34], internal oxidation [35] and a special thin-film technique [37, 38]. The morphology in all 7 systems is governed by the formation of (111) interfaces, which indicates that the (111) boundaries have the lowest energy. For the Ag/Ni system this confirms the results from embedded atom calculations by Gao et al. [8]. An interesting observation, which is consistent with the values obtained in calculations of interfacial energies, is the

decomposition of a (110) interface in Ag/Ni into atomic-scale microfacets, producing a sawtooth-like configuration of (111) boundaries [37]. That dense-packed planes form low energy interfaces has been suggested by the work of Wolf [18, 19, 21, 39].

6.2 Misfit Localization

Figure 4 shows a (111) interface of a Cu precipitate, viewed along $<1\bar{1}0>$. Although the misfit is quite large (η=0.14), a definite modulation in the structure of the interface can be observed. The spacing corresponds to the expected spacing of misfit dislocations. The core of the misfit dislocations is somewhat delocalized, involving about 3 (111) planes on the Cu side. It also appears that Cu planes in the core do not fully meet the NiO plane, but end at roughly one interplanar spacing from the (111) NiO plane. Such an introduction of vacancy-type defects may be able to minimize the interfacial energies for large misfit boundaries that have strong enough bonding that coherence is maintained over part of the interface. A different kind of standoff behavior was first observed for the Nb/Al_2O_3 interface [40]. In this case the energy of the interface is minimized by maintaining perfect coherence for the first metal layer, while the misfit dislocation is formed at some distance from the interface.

Misfit dislocations on (111) heterophase boundaries are expected to form a hexagonal network, as observed for example in the epitaxy of Pd on Au [36]. Here edge type dislocations of Burgers vector b=a/2<011> with line vectors <211> form a network of dislocations, two of which are inclined by 30° to the <011> HREM viewing direction and one of which is perpendicular to <011>. Obviously, atomic relaxations that vary with depth and are normal to the beam direction will disturb the "atom-like" HREM features that represent atomic columns in HREM images. We can distinguish three regimes depending on the magnitude of the misfit, or in other words, the size of the planar unit cells that define the two-dimensional network of interfacial relaxations. When the misfit is large, the

dimension of the network of relaxations is smaller than the typical thickness of a HREM specimen. Therefore, the atomic column contrast is disturbed due to this variation of relaxations within the sample thickness. However for very large misfits (~0.15, see fig.4), due to St. Venant's principle, the disturbance is very local and atomic column contrasts will still be observed quite close to the interface. For intermediate misfits, such as in fig.5, which shows a NiO precipitate in a Pd matrix, at a misfit η=0.07, the strain fields are more extended and consequently the effects on the column contrast are also more pronounced. Finally, at quite small misfits, such as in the NiO/Ag interface in fig.6 (η=0.02), the planar unit cell of the relaxations cannot be contained within the thickness of the specimen whenever the spacings between misfit dislocations is on the order of 10 nm or larger. In this event local variations of relaxations in depth are only important near the misfit dislocation running through the thickness of the foil. Although the true nature of the misfit defect may still be obscured, the presence and location of the misfit can clearly be observed. Within each of these regimes the strength of the interatomic bond at the heterophase boundary and the elastic constants within both media will have a strong effect on the actual atomic arrangements and relaxations.

Although HREM observations of heterophase boundaries in fcc systems have so far been rather qualitative, an important result is the presence of misfit localization in practically all systems, even for quite large misfits [35]. Structural details, such as the standoff effect for misfit dislocations, which has now also been observed in fcc systems (see fig. 6) [37], will affect interfacial properties. As for the Nb/Al_2O_3 interface, the standoff distances observed in Ag/NiO and Au/NiO are also in agreement with the elastic model by Kamat et al.[41].

The Ag/Ni interface is an important model system for metallic heterophase boundaries, since the constituents are mutually insoluble and the misfit is extremely large (η=0.15). While conventional TEM does not suffice for the detection of misfit dislocations

in this system [42], HREM has clearly shown misfit localization [37, 38]. The misfit dislocation in the Ag/Ni interface in fig. 7 is somewhat delocalized. This can be compared to the relaxations calculated by Gao et al. using embedded atom potentials [8]. Based on this computer simulated (111) Ag/Ni interface the image simulations in fig. 7b show reasonably good agreement with the experimental images.

6.3 Interface Bonding

The chemical nature of the atoms situated at or near the interface and their mutual interactions are of prime importance for determining properties and structures of interfaces. HREM can in some instances be utilized to obtain chemical information. Detailed HREM images may reveal the chemical nature of the interface atoms, as studied, for example, by Necker and Mader who compared possible models for the terminating plane with observations [43]. NiO precipitates formed by internal oxidation in Pd grow with almost equal probability in the cube-on cube orientation and the twin related orientation, where the stacking sequence on (111) planes is reversed (compare figs. 4a and 4b) [35]. This behavior could be explained if the interatomic interactions across the interface are extremely short range, i. e. if second nearest neighbor interactions can be neglected. Although there exist no calculations for this particular geometry, there are indications from electronic structure and total energy calculations of metal/ceramic interfaces, that the interface effect can be limited to the interface layer [22]. It should be noted that the bonding across a metal/ceramic interface is dependent not only on the type of atoms involved, but even in nonreactive systems, the bonding will depend on the defect state, (which can be controlled, for example, by the oxygen partial pressure during manufacture) and impurity segregation effects. Therefore, HREM has to be augmented by techniques (such as the atom-probe field-ion microscope) that can identify point defects and impurities.

6.4 Summary - Heterophase Boundaries in fcc Materials

Low-energy interfaces are the (111) planes. Some degree of misfit localization has been found in practically all systems. The presence of misfit dislocations, even at large misfits and for weakly bound systems, is of importance for interface properties, such as mechanical properties and impurity segregation. It appears that the misfit localization is a result of maximizing the areas of good atomic fit across the interface. The stand-off effect for misfit dislocations is also present in fcc systems, and is expected for all situations, where the misfit dislocations are located in the softer material [37].

Whenever misfit localization occurs, HREM is difficult to apply to phase boundaries in fcc systems, since the translational symmetry of the lattice in the direction of the electron beam is not maintained near the interface. Because of the difficulties in deconvoluting the three-dimensional relaxations near the interface and the scarcity of suitable theoretical models, particularly for metal/ceramic boundaries, the investigations to-date have largely been qualitative. Nevertheless, the HREM technique, when applied in conjunction with model calculations, holds great promise, also for the quantitative investigation of interfacial structures in heterophase systems.

7. HREM of Grain Boundaries in Ceramics and Metals

In contrast to heterophase boundaries, tilt GBs can be considered as ideal systems for investigations by HREM, since the translational symmetry along the tilt axis typically is not expected to be destroyed by the atomic relaxations near the GB. Therefore, although reconstructions within the GB core are possible and could complicate the simple picture of rigid atomic columns being displaced normal to the tilt axis [30], images of tilt GBs along a low-index direction usually can be analyzed in terms of rigid atomic columns.

The cubic transition metal oxides, which are typically insulators or wide-bandgap semiconductors, represent a widely different class of materials, compared to close-packed metals. The interatomic interactions in both types of materials are quite different, but in contrast to metal/ceramic interfaces, both the Coulomb interaction in mostly ionic oxides, and the interatomic interactions in fcc metals are reasonably well understood. Therefore, these materials , such as NiO, which has the rock-salt structure (strictly speaking above the Néel temperature , ~ 210 °C, with a minute rhombohedral distortion below this temperature) or Au, as an fcc metal, can be treated by atomistic simulation with realistic interatomic potentials. Both materials, which we use as model substances, are close-packed fcc solids. The largely ionic interactions in NiO puts severe constraints on the arrangements of atoms at lattice defects, such as a GB. Basically, configurations which place like charges into close proximity must be avoided, since due to the strong Coulomb interaction, such arrangements are energetically extremely unfavorable. Therefore, ionic oxide GBs are expected to have a more open structure than corresponding configurations in metals [44, 45]. For fcc metals, simple two-body potentials are often used for GB simulations, the introduction of the embedded atom method [46] also allows the effect of the electronic redistributions at interfaces to be taken into account, and these potentials are therefore believed to give more realistic results than simple two-body potentials.

In the following we shall review a few selected results of our HREM investigations in NiO and Au grain boundaries. The experiments involved the preparation of bicrystals of the desired orientation. The NiO specimens were prepared from bulk bicrystals [47], while the Au samples were prepared by a thin-film technique [48, 49].

7.1 Atomic-scale Faceting

Grain boundaries are generally strongly faceted in NiO as well as Au. The fact that *planar* facets are formed indicates that low energy interfaces are planar, that certain GB

inclinations are energetically preferred over others, and that only a finite set of GB inclinations is energetically possible. Figure 8 illustrates the facets found in a small island grain in Au (θ=50.5°, Σ=11). The two symmetric GBs, which are situated at an inclination of 90° to each other are connected by asymmetric facets. The well-structured symmetric (113)(113) GB at the top and bottom of fig.8, has the greatest facet length, which would be expected, since it is well known that this GB (which is characterized by the second most dense plane in the fcc structure on which a symmetric tilt GB can be formed) is connected with a deep energy cusp [50]. Atomic-level observation of facets is important since it allows us, as closely as possible, to identify the crystallographic planes involved in the formation of the interface. At lower resolution, the apparent inclination of a GB is not necessarily the true inclination. The average boundary orientation could, for example, be influenced by regular arrangements of atomic-scale steps, or by the reconstruction into atomic-scale facets. The latter mechanism has in fact been invoked in the past by suggestions that asymmetric GBs may consist of symmetric facets [51, 52].

Our observations in NiO as well as in Au show, for all misorientations investigated, coexistence of symmetric and asymmetric GBs. In many instances, asymmetric GBs seem to be preferred energetically. This is indicated by extended facets observed, particularly for GBs incorporating one or two low-index planes [47, 53 -55]. Recent computer simulation studies of symmetric and asymmetric GBs in Au have indeed shown, that in many instances, asymmetric GBs have lower energies than the corresponding symmetric GBs [56]. On the basis of our observations and the computer simulations we believe this to be a general property of GBs in cubic systems.

7.2 Grain Boundary Core Structure

Potentially a critical test for atomistic calculations of large-angle tilt GBs is the detailed comparison to HREM observations of atomic core structures. While there are some quite detailed investigations for covalent solids, to-date few comparisons with simulated structures have been made for fcc systems. Qualitative agreement with calculations has been reported for short-period boundaries in Au [57-60] . In NiO, both the Σ=5, (210) and (310) GBs show strong deviations from the calculated structures, while the observed structure for the Σ=13, (320) GB is in qualitative agreement with the calculated structure [44, 47, 61, 62]. Although the NiO GBs generally appear to have a more open structure than the metallic GBs, the Σ=5 GBs have a quite dense arrangement of atomic columns, essentially containing one additional atomic plane (or one extra atomic column per structural unit, see fig. 9), compared to the calculations by Duffy and Tasker [44]. The rigid-body displacement normal to the GB, the so-called volume expansion, for the (310) GB is approximately 0.3 Å, compared to 1.1 Å for the calculated structure [61]. The total excess volume of the boundary may however be greater than given by the rigid-body shift, when vacancy-type defects are present at the GB. Some or all of the atomic columns at the interface would then not be fully occupied. The strong Fresnel contrast behavior which is invariably observed for these GBs indicates that this is indeed the case in NiO. Consequently, HREM images should be expected to reflect the partial occupation of columns. Figure 10 compares the image simulations of a (310) GB in NiO with fully dense atomic columns with a boundary whose core is surrounded by atomic columns containing 25% vacancies. Although the differences between HREM images are quite clear (especially when viewed with a false color palette), subtle contrast effects at the interface may also be caused by small variations in specimen thickness, since the latter is only approximately 10 lattice parameters. Therefore HREM must be supplemented by other techniques, such as Fresnel contrast and small angle x-ray scattering for the determination

of the excess volume in the presence of point defects at the GB [63]. Atomistic computer simulation studies of twist GBs in NiO have suggested that a reconstruction which amounts to the introduction of Schottky pairs, greatly stabilizes such boundaries [64, 65]. It appears that incorporation of vacancy-type defects into the GB structure may also be important for tilt GBs in ceramic oxides.

In contrast to oxides, which can contain large concentrations of point defects and deviations from stoichiometry, concentrations of point defects large enough to affect GB structure are not expected in metallic GBs. GB computer simulations of a wide range of GBs for fcc metals have recently been performed by Wolf, using simple two-body, as well as embedded atom method (EAM) potentials. Rather universal correlations are found between GB energy and volume expansion, and atomic coordination at grain boundaries [20, 21]. Both of these quantities should be accessible by HREM. At this point, a few comparisons between the measured and theoretical volume expansions have been made. While the measured volume expansions for Al agree well with EAM calculations [66], experimental values for Au are significantly larger (typically a factor of two) than the values obtained from EAM calculations [60, 67]. The origin of this discrepancy is not known at the moment. When measuring rigid-body displacements, the core region and the atomic planes in its vicinity, affected by elastic distortions, must be excluded. In contrast to α-fringe methods which can very accurately determine relative displacements [68], HREM, which allows identification of the atomic columns in the core, is essential for obtaining absolute measurements of the rigid-body displacements [69].

That there are significant deviations between observed and calculated GB expansions for both NiO and Au is somewhat disappointing, since computer simulations indicate that this parameter is directly correlated to GB energy and could thus serve as an experimentally measurable indication for the magnitude of GB energy. There are several possible effects that could contribute to the observed deviations between calculations and

experimental determination of the volume expansion. Clearly, calculations for 0 K may not directly be applicable to structures that were manufactured at elevated temperature. Entropic effects, especially in NiO, should also be taken into account. It should also be noted that the calculations typically refer to the relaxation of fully dense planes. However, when reconstruction is possible, i. e. when point defects are introduced or when the translational symmetry in the direction of the tilt axis is not maintained, completely different structures may be formed. As for Au, it is surprising that the EAM potential, which explicitly takes into account electronic relaxations in GB cores, gives not as good an agreement than the simple two-body Lennard-Jones potential. Different fcc metals need to be investigated in order to establish the reliability of potentials and calculations to predict experimental structures. Finally, calculations will need to take into account thermodynamic factors, by simulations at finite temperatures. Experimentally, the effects of impurities on structure must also be investigated.

7.3 Structural Multiplicity

While the rigid-body translation normal to the GB is strongly connected to GB energy, several translational states parallel to the GB may correspond to local minima in GB energy. This is in fact typical for lattice statics calculations, and therefore, multiple structures had been predicted, based on GB computer simulations [70]. When the energies for different translational states are identical, or close together, it is expected that such boundaries coexist. Figure 11 a) shows , for the same Σ=5, (310) macroscopic GB plane orientation, two different core structures in NiO, side by side. A small step between the two facets, separates the two GB planes by a distance of ~0.2 nm.. Whenever the relative atomic pattern on both sides of the boundary changes by such a shift of the boundary plane, or in other words when the step is not a multiple of the corresponding interplanar spacing of the CSL, a different core structure results. This movement of the GB plane is

equivalent to a rigid-body translation parallel to the GB plane, as illustrated schematically in fig. 11 b).

Structural multiplicities add greatly to the possible atomic scale configurations of a GB. Multiple structures have also been observed in Au for the (113) and (221) STGBs [67]. The structure with mirror symmetry is generally not the preferred structure. In Au, structural multiplicity has also beeen observed in asymmetric GBs [56]. Therefore, structural multiplicity for the same macroscopic GB configuration , appears to be a quite general phenomena. It should be noted, that in real crystals, and especially in nanophase aggregates, and for finely faceted boundaries, the GB translational states for some facets may be constrained. Therefore a still wider spectrum of translational states may be present in finely grained materials.

7.4 Asymmetric Grain Boundaries

Tilt bicrystals typically contain many different kinds of facets. It was first noticed on <001> tilt GBs in NiO that the boundary plane frequently assumed asymmetric configurations. Facets that included one low-index plane in particular (i. e. a plane with relatively dense atomic packing) seemed to be preferred [54]. The coexistence of symmetric and asymmetric facets, which is observed for all misorientations in NiO and Au, suggests that the energies of symmetric and asymmetric GBs are for most bicrystals not too much different. Since for each tilt misorientation there are at most two crystallographically different symmetric facets in a given bicrystal, while an infinite number of asymmetric boundaries is geometrically possible, asymmetric boundaries may dominate the properties of polycrystals.

In order to establish the role of the GB plane concerning GB energy, HREM observations in Σ=9 and Σ=11 bicrystals were recently combined with computer simulations of GBs in these systems. The results of the simulations showed indeed that

many asymmetric GBs were lower in energy than the corresponding symmetrical GBs [56]. Experimentally, in agreement with the GB-energy calculations, no particular facet was preferred over others, except for the case of the (113)(113) GB, which is well known to be associated with a deep cusp in GB energy [50]. Figures 12 and 13 show examples of the coexistence of symmetric and asymmetric facets for the Σ=9 and Σ=11 bicrystals, respectively. The *planar* (111)(115) asymmetric tilt GB is according to the simulations the second lowest in energy for the Σ=9 bicrystal (after the (001)(447) GB), nevertheless, fig. 12 shows instead of a single, *planar* facet, the well-known dissociation of this boundary into triangular regions [71-74], bounded by two (111)(111) and one (112)(112), Σ=3 twins. When the calculated energies of all of the Σ=3 twin boundaries are added up, and normalized to the area of a planar interface, this total energy is indeed lower than the energy for the *planar* (111)(115) interface [56]. On the right hand side of fig. 13, a (111) plane is almost parallel to the GB in one of the crystals, the boundary on the left is the symmetric (114)(114) GB, with its relatively short structural units. Although the Σ=9 misorientation does not allow (111) and (110) planes to be exactly parallel, short facet steps are often formed near these planes, indicating that there is a tendency toward relaxations which involve two low index planes.

In the Σ=11 bicrystal in fig. 13 (which depicts an enlarged section of fig. 8) the GB planes range from (113)(113) to (225)(441), (557)(771), and (332)(332). The (113)(113) STGB shows the longest facet and the smallest structural repeat unit. The asymmetric facets show considerable asymmetries in their atomic structures. While on the inside of the island grain (bottom right in fig. 13), the lattice appears relatively undisturbed even quite close to the GB, strain fields with the periodicities of the structural units are clearly visible at the exterior of the grain.

When the misorientation between the two grains allows two low index planes to be parallel to each other, grain boundaries at these inclinations are clearly preferred. The

formation of long, asymmetric facets of such boundaries indicates that their energy is particularly low compared to other inclinations. Examples are the (111)(100) GB which is formed in Au at θ=54.74° , $<1\bar{1}0>$ (which is quite close to Σ=41, θ=55.88°), and the (100)(110) and (100)(210) GBs in NiO at θ=45° and θ=26.6°, <001>, respectively. The coexistence of symmetric and asymmetric facets in NiO as well as in Au, and the tendency for the formation of GBs which incorporate low-index planes, suggests that low-energy GBs in fcc systems can assume a considerable variety of structures, which, however, appear to have a tendency to form dense-packed atomic arrangements.

7.5 Atomic Matching

For small-angle GBs, coherence between the two lattices is maintained in between regions of misfit characterized by primary GB dislocations. While small-angle GBs are well described by the Read-Shockley model, it is much less clear to what extend, if at all, atomic matching across large-angle GBs plays a role. In fact, some large-angle GBs, such as in figs. 9 and 11 can be considered incoherent. The geometric match between certain atomic sites in the GB, which is established for CSL orientations, is destroyed when the bicrystal undergoes a rigid-body translation [75]. However, many GBs in NiO, Au and other materials show atomically well-matched regions for many high-angle GBs. Atomic matching can be understood as having a GB region in which the relaxed atomic structures form a smooth transition between lattice 1 and lattice 2. Such matching between the two lattices can be best recognized by an apparent elastic continuation of low-index atomic planes across the GB, which then may be considered semicoherent. It would appear that well-matched regions should be accompanied by low interfacial energies. Observation of extended facets with atomically well-matched interfaces for many bicrystals in Au support such a view. Recent embedded atom calculations by Wolf on metal GBs have indeed

indicated a general correlation between the average degree of atomic coordination in the boundary and GB energy [20, 21, 76].

The idea that large-angle GBs may consist of regions of good match, followed by regions of poor match goes back to a suggestion by Mott [77]. For periodic GBs, when the planar unit cell is small, the GB period can be extremely small, such as in the Σ=5 GBs (see figs. 9 and 11). In this case the rigid-body translation prevents the continuation of low index lattice planes across the GB in the sense discussed above. However, most large-angle GBs have considerably larger structural units. Therefore local relaxations may lead to misfit localization within the planar unit cell with the concomitant formation of well-matched regions. Figure 14 presents an example of such a boundary in Au. In this (443)(443) GB we clearly see the misfit localization within the structural units of this boundary, as well as the continuation of low index planes across a large fraction of the planar unit cell. In addition to this, the compressed image of this boundary indicates at the core a continuous arrangement of corrugated, dense-packed "planes "on both sides of the boundary. It appears that there is a tendency to retain as much as possible the atomic coordination of the ideal crystal and that these structures have developed through relaxation of the dense-packed (111) planes which form a shallow angle to both sides of the GB plane. A particularly well-matched structure is given by the (113)(113) GB in fig. 13, which shows good continuation of three sets of low-index planes in addition to having a very small structural repeat distance. By contrast, the other symmetric GB for Σ=11, i.e. the (332)(332) (situated at 90° to the (113)(113) GB in fig.13) can be considered incoherent.

For NiO well-matched boundaries are also found, when the structural repeat period is not too small. Examples are the Σ = 13, (510) GB shown in fig. 15 a which clearly includes regions with good atomic match in between regions of poor match. Figure 15b illustrates another such case for the (320) GB which has the same misorientation angle as

the (510) GB. In this case we find closely spaced, well matched regions for which a good continuation of (220) planes across the GB can be observed by HREM.

Observation of a number of fcc boundaries indicates, that whenever possible, atomically well-matched regions are formed. This tendency to maintain, as much as possible, the local atomic environment of the lattice, can be quantified, utilizing HREM information on atomic positions at GBs. Such an investigation is underway and its results should be of particular interest for comparisons to the broken bond model, which establishes a direct connection between GB miscoordination and GB energy [76].

7.6 Quasiperiodic Grain Boundaries

As discussed in section 4. perfectly periodic grain boundaries (but extending over a finite distance in real crystals) are only possible for very special (i. e. the CSL) misorientations. Aperiodic features may be introduced by deviations from the exact coincidence misorientation angle or by forming boundaries on irrational planes. Theoretically it has been shown that such irrational GBs can be considered quasiperiodic, in analogy with the structures of quasicrystalline materials [9, 10, 78].

Another type of quasiperiodicity can be formed when the atomic relaxations are such that smaller structural units are formed than given by the CSL period (for an illustration of this, see fig. 2). The $<1\bar{1}0>$ tilt GB (θ=55°) in fig.16 is very close to Σ=41 (θ=55.88°) and a boundary , which has (111) and (001) planes exactly parallel to each other (θ=54.74°). The GB in fig. 16 can be approximated in the CSL description by (23,23,24)(001) with a structural repeat period of 11.8 nm, while the interatomic distances along the (111)(001) planes and perpendicular to the tilt axis are incommensurate. This boundary displays atomically well-matched regions that are separated by less well coordinated areas. The compressed image in fig. 16 indicates that slight elastic distortions

of the lattice on both sides of the GB accompany the misfit localization. The period of these features is approximately 1.8 nm. This is the exact analogue to the formation of misfit dislocations in heterophase boundaries. The misfit in the distances between atomic columns along the <110> and <121> directions for the (001) and (111) planes respectively is being accommodated by misfit-dislocation-like defects. The misfit in this case is 14 %, while the period, determined for a rigid model is approximately 1.86 nm, in agreement with the observation. In contrast to heterophase interfaces, the periodicity of the lattice is maintained in the direction of the tilt axis, therefore the atomic columns are quite sharp and distinct right up to the GB. Such misfit-dislocation-like structures are ideally suited for HREM analysis.

This observation of one-dimensional quasiperiodicities in tilt GBs shows the ability of the lattice to seek out relaxation modes that do not necessarily maintain the symmetry of the bicrystal, but rather assume local atomic arrangements that maintain, as much as possible, the atomic coordination of the lattice. When a GB consists of dense-packed planes it most often forms an interface that is quasiperiodic in at least one direction. Moreover, the extended facets that have been observed for the (111)(001) interface indicate that this GB has quite low energy. Observation of this boundary geometry in other systems and the observation that (001) surfaces in Au reconstruct into the same geometry, supports this conclusion [79, 80].

We believe that quasiperiodicities also exist in oxide GBs, where the frequent formation of GBs that contain at least one low-index plane was first observed. An example of a GB bounded by two incommensurate planes is given in fig.17, which shows the (210)(100) GB in NiO (see also fig.2). In this HREM micrograph the elastic distortions are not apparent, however misfit localization also seems to be present, although in a more disordered fashion compared to Au.

While asymmetric GBs may often be incommensurate, symmetric tilt GBs are always commensurate and their structural repeat periods should therefore always be governed by the bicrystal geometry. Quasiperiodicities for tilt GBs would then only arise due to deviations from exact CSL orientations, and the quasiperiod would be long compared to the corresponding CSL unit. However we have recently found a different kind of quasiperiodicity, which we believe is due to fluctuations, possibly caused by entropic effects. Fig. 18. shows a symmetric, large-angle GB that has an interesting 3-dimensional nature given by the stacking disorder, which extends to a short distance from the GB for, on average, every 15 (111) planes crossing the GB. It can clearly be seen in fig.18 that the spacing between stacking faults is not strictly periodic, but varies by a few (111) planes. Since the GB is symmetric, and is within less than 1° of the Σ=41 orientation, one would expect that the structural units of this GB would be identical in size to the distance between CSL points on the (338) plane. However the structural repeat distance for the CSL boundary is 2.6 nm, compared to the average distance between stacking faults of 3.6 nm. Obviously, this GB is not governed by the Σ=41 geometry. However, this GB can be considered vicinal to the (113)(113) GB (θ=50.5°), where the additional 5° misorientation is accommodated by the stacking faults protruding from the interface. This novel kind of three-dimensional GB structure may be limited to materials with a low stacking-fault energy. Therefore, it should be interesting to investigate the structures that develop for the same macroscopic geometry in fcc metals which have a much higher stacking-fault energy than Au.

The reason why quasiperiodic structures are formed for this GB is probably due to the quite low energies associated with the stacking disorder in Au. Therefore, during formation, possible residual stresses and entropic effects could have been sufficient to generate these deviations from periodicity.

While tilt GBs can in principle have perfect translational symmetry in the direction parallel to the GB and perpendicular to the tilt axis, at least for certain misorientations and GB planes, HREM has shown that the atomic relaxations at interfaces can lead to structures that are quasiperiodic. The origin of the deviation from periodicity can be due to misfit localizations along incommensurate planes or result from inhomogeneities or fluctuations present during the formation of the interfaces.

7.7 Summary- Grain Boundaries in fcc Materials

HREM observations have been invaluable for investigations of the atomic structure of GBs in fcc ceramics and metals. A number of structural features of GBs are common to NiO and Au, and are expected also to apply to fcc materials in general. Among those we note:

1. GBs form rather dense, well-structured atomic arrangements in the form of planar facets.
2. For each bicrystal there is a finite number of GB plane orientations (inclinations).
3. Symmetric and asymmetric facets coexist.
4. Asymmetric facets often appear to have similar or lower energies than the symmetric ones.
5. GBs incorporating low-index (i. e. atomically dense packed) planes appear energetically preferred.
6. In symmetric as well as asymmetric GBs multiple core structures can exist for the same macroscopic geometry.
7. Symmetric GBs generally do not have mirror symmetry.
8. Misfit localization and atomically well-matched regions are a common feature of large-angle GBs.

9. Boundaries formed on incommensurate planes are quasiperiodic due to misfit localization.

Atomic structure comparisons show that available theoretical GB models are not fully satisfactory. The purely geometrical models not only fail, as expected, in making predictions concerning the interfacial energy, but they also can not always uniquely predict the relevant structural periodicities. Atomistic calculations based on EAM potentials are in good agreement with observations for Al, while in Au much larger than theoretical volume expansions are found. The observed structures have in some instances considerably smaller rigid-body translations normal to the GB than predicted for NiO by lattice-statics calculations. It appears that tilt GBs in ionic oxides may reconstruct by incorporation of vacancy-like defects into the GB.

HREM observations of tilt GBs in Au have revealed several novel GB structures. This has shown that there is a great variety of possible atomic relaxations even in simple fcc materials. Further progress in our understanding of GBs will need the combined application of theoretical and experimental techniques. Refinement of theoretical approaches by incorporating the effects of finite temperature, for example, and more detailed and systematic HREM investigations that allow direct correlations to atomistic GB parameters will be needed for obtaining a more complete understanding of GBs on an atomic level. The latter is well recognized to hold the key to the understanding and improvement of many important properties of materials.

8. Summary and Conclusions

HREM investigations in fcc materials have provided a wealth of new insights into the atomic structure of hetero- and homophase boundaries.

HREM has clearly demonstrated that a universal tendency exists to produce atomically well-matched structures and to preserve a high degree of coherency across the interface. It has been shown that misfit localization occurs to very large values of misfit in several heterophase systems. HREM observations have established that misfit-dislocation-like defects also are formed in large-misfit, incommensurate grain boundaries. Thus a direct connection has been made between the two traditionally separate fields of phase boundaries and grain boundaries. In fact, the tilt-GB-type misfit dislocations represent ideal objects for HREM studies of misfit localization. It has become clear that atomic relaxations behave qualitatively similar in these different systems. One important conclusion is that atomic relaxations are quite local and that *very* long periods or quasiperiodicities, determined by the bicrystal symmetry, may be quite irrelevant to the actual grain boundary structures.

We conclude that the complementary capabilities of HREM experiments and atomistic computer simulations are necessary to obtain a full understanding of the correlation between interface structures and properties. While for grain boundaries, HREM experiments are essentially limited to the exploration of tilt boundaries, atomistic computer simulations are basically limited to periodic boundaries, but can investigate much of the five-parameter misorientation phase space associated with the macroscopic degrees of freedom of a grain boundary. Since there is such a great variety of possible structures, the mutual feedback between theory and experiment is important, not only for establishing the validity of potentials and relaxation procedures, but also for elucidating the essential aspects of interfacial correlations.

Extensive computer simulations have suggested direct correlations between GB energy and i) the rigid-body translation normal to the GB and ii) the number of broken bonds per GB unit area. Therefore important areas of future work are systematic HREM investigations of these GB parameters. Combined with the simulations, HREM measurements of the volume

expansion and the miscoordination coefficients thus provide information on GB energies. In addition, the length of facets in bicrystals can also be related to relative GB energies in bicrystals.

For the determination of the total excess volume in oxide GBs in the presence of GB reconstruction (i. e. incomplete occupation of atomic columns at the GB) HREM will have to be supplemented by additional techniques, such as the Fresnel contrast technique, while GB calculations will have to include the effects of temperature and the influence of point defects. It is expected that the symbiotic relationship between HREM observations and computer simulations will result in a much refined understanding of interfaces on an atomic scale.

Acknowledgements. The author would like to thank his collaborators, particularly D. J. Smith for his contributions to the work on NiO, and Y. Gao and B. Shao for their work on heterophase interfaces. I also would like to express my thanks for the technical assistance by J. F. Reddy and C L. Wiley, and for many helpful discussions with W. Mader, L. D. Marks, D. N. Seidman, D. A. Smith, and D. Wolf. The National Facility for HREM in the Center for Solid State Science at Arizona State University and the Department of Materials Science & Engineering at Northwestern University are gratefully acknowledged for making the JEM4000 (ASU) and the H9000 (NWU) available for this research. This work was supported by the U. S. Department of Energy, Basic Energy Science- Materials Sciences, under Contract No. W-31-109-Eng-38.

References

[1] J. C. H. Spence, Experimental High-Resolution Electron Microscopy, *2nd Edition* (Oxford University Press, New York, Oxford, 1988).

[2] High-resolution electron microscopy and associated techniques, EDs P. R. Buseck, J. M. Cowley, and L. Eyring (Oxford University Press, New York, Oxford, 1988).

[3] A. Bourret, Colloque de Phys. 51 (1990) C1-1.

[4] A. Bourret and J. L. Rouvière, in Polycrystalline Semiconductors, Springer Proceedings in Physics 35, (Springer-Verlag, Berlin, 1988) p. 8.

[5] D. Wolf and J. F. Lutsko, Zs. f. Kristall. 189 (1989) 239.

[6] M. Weins, H. Gleiter, and B. Chalmers, J. Appl. Phys. 42 (1971) 2639.

[7] R. W. Balluffi, A. Brokman, and A. H. King, Acta metall. 30 (1982) 1453.

[8] Y. Gao, P. G. Shewmon, and S. A. Dregia, Acta Met. 37 (1989) 3165.

[9] N. Rivier and A. J. A. Lawrence, Physica B 150 (1988) 190.

[10] A. P. Sutton, Acta Met. 36 (1988) 1291.

[11] J. W. Matthews, in Epitaxial Growth, Ed. J. W. Matthews (Academic Press, 1975) p. 559.

[12] J. H. van der Merwe, J. Appl. Phys. 34 (1963) 117.

[13] J. H. van der Merwe, J. Appl. Phys. 34 (1963) 123.

[14] G. B. Olson and M. Cohen, Acta Met. 27 (1979) 1907.

[15] R. Bonnet and F. Durant, Phil. Mag. 32 (1975) 997.

[16] R. Bonnet, Mat. Res. Soc. Proc. 122 (1988) 281.

[17] A. P. Sutton and R. W. Balluffi, Acta Met. 35 (1987) 2177.

[18] D. Wolf, Acta Met. 37 (1989) 1983.

[19] D. Wolf, Acta Met. 37 (1989) 2823.

[20] D. Wolf, Acta Met. Mater. 38 (1990) 781.

[21] D. Wolf, Acta Met. Mater. 38 (1990) 791.

[22] A. J. Freeman and C. Li, in Metal-Ceramic Interfaces, EDs. M. Rühle, A. G. Evans, M. F. Ashby, and J. P. Hirth, (Pergamon Press, 1990) p. 2.

[23] P. Blöchl, G. P. Das, H. F. Fischmeister, and U. Schönberger, in Metal-Ceramic Interfaces, EDs. M. Rühle, A. G. Evans, M. F. Ashby, and J. P. Hirth, (Pergamon Press, 1990) p. 9.

[24] M. W. Finnis, A. M. Stoneham, and P. W. Tasker, in Metal-Ceramic Interfaces, EDs. M. Rühle, A. G. Evans, M. F. Ashby, and J. P. Hirth, (Pergamon Press, 1990) p. 35.

[25] M. F. Ashby, F. Spaepen, and S. Williams, Acta Met. 26 (1978) 1647.

[26] International Conference on the Structure and Properties of Internal Interfaces, EDs. M. Rühle, R. W. Balluffi, H. Fischmeister, and S. L. Sass, Journ. de Physique 46, (Colloque C4, 1985) .

[27] Grain Boundary Structure and Related Phenomena, Ed. Y. Ishida, Transactions of the Japan Institute of Metals 27, (1986) .

[28] Interface Science and Engineering '87, EDs. R. Raj and S. L. Sass, Journ. de Physique 49, (Colloque C5, 1988) .

[29] Intergranular and Interface Boundaries in Materials, Colloque de Physique 51, (Les Éditions de Physique, 1990) .

[30] S. M. Foiles, M. I. Baskes, and M. S. Daw, Mat. Res. Soc. Symp. Proc. 122 (1988) 343.

[31] C. Anterroches, P. Perret, and J. R. Brosselin, Colloque de Phys. 51 (1990) C1-729.

[32] U. Dahmen, M. J. Witcomb, and K. H. Westmacott, Colloque de Phys. 51 (1990) C1- 737.

[33] see for example, Metal-Ceramic Interfaces, EDs. M. Rühle, A. G. Evans, M. F. Ashby, and J. P. Hirth, Acta-Scripta Metallurgica Proceedings 4, (Pergamon Press, 1990) .

[34] K. L. Merkle and B. Shao, Mat. Res. Soc. Symp. Proc. 122 (1988) 69.

[35] K. L. Merkle, in Metal-Ceramic Interfaces, EDs. M. Rühle, A. G. Evans, M. F. Ashby, and J. P. Hirth, (Pergamon Press, 1990) p. 242.

[36] G. Honjo and K. Yagi, in Current Topics in Materials Science, 6 EDs. E. Kaldis (North-Holland, 1980) p. 195.

[37] Y. Gao and K. L. Merkle, J. Mater. Res. in press (1990).

[38] Y. Gao and K. L. Merkle, Mat. Res. Soc. Proc. (1990) in press.

[39] D. Wolf, J. de Physique 46 (1985) 197.

[40] W. Mader and G. Necker, in Metal-Ceramic Interfaces, EDs. M. Rühle, A. G. Evans, M. F. Ashby, and J. P. Hirth, (Pergamon Press, 1990) p. 223.

[41] S. V. Kamat, J. P. Hirth, and B. Carnahan, Mat. Res. Soc. Symp. 103 (1988) 55.

[42] P. Gumbsch, R. Maurer, and H. F. Fischmeister, Mat. Res. Soc. Symp. Proc. 122 (1988) 67.

[43] G. Necker and W. Mader, Phil. Mag. Lett. 58 (1988) 205.

[44] D. M. Duffy and P. W. Tasker, Phil. Mag. A 47 (1983) 817.

[45] D. M. Duffy and P. W. Tasker, Phil. Mag. A 48 (1983) 155.

[46] S. M. Foiles, M. I. Baskes, and M. S. Daw, Phys. Rev. B 33 (1986) 7983.

[47] K. L. Merkle and D. J. Smith, Ultramicroscopy 22 (1987) 57.

[48] T. Schober and R. W. Balluffi, Phil. Mag. 21 (1970) 109.

[49] T. Y. Tan, J. C. M. Hwang, P. J. Goodhew, and R. W. Balluffi, Thin Solid Films 33 (1976) 1.

[50] G. Hasson, J.-Y. Boos, I. Herbeuval, M. Biscondi, and C. Goux, Surface Science 31 (1972) 115.

[51] M. S. Masteller and C. L. Bauer, Phil. Mag. A 38 (1978) 697.

[52] A. Brokman, P. D. Bristowe, and R. W. Balluffi, Scripta Met. 15 (1981) 201.

[53] K. L. Merkle, in Proceedings of the 46th Annual Meeting of EMSA, Ed. G. W. Bailey (1988) p. 588.

[54] K. L. Merkle, J. F. Reddy, C. L. Wiley, and D. J. Smith, in Ceramic Microstructures '86, EDs. Pask and Evans (1987) p. 241.

[55] K. L. Merkle, Mat. Res. Soc. Symp. Proc. 153 (1989) 83.

[56] K. L. Merkle and D. Wolf, to be published (1990) .

[57] Y. Ishida, H. Ichinose, M. Mori, and M. Hashimoto, Trans. Jap. Inst. Met. 24 (1983) 349.

[58] W. Krakow, J. T. Wetzel, and D. A. Smith, Phil. Mag. A53 (1986) 739.

[59] F. Cosandey, S. W. Chan, and P. Stadelmann, Scripta Met. 22 (1988) 1093.

[60] F. Cosandey, S.-W. Chan, and P. Stadelmann, Colloque de Phys. 51 (1990) C1-109.

[61] K. L. Merkle and D. J. Smith, Phys. Rev. Lett. 59 (1987) 2887.

[62] K. L. Merkle, J. F. Reddy, C. L. Wiley, and D. J. Smith, J. de Physique 49 (1988) 251.

[63] C. B. Boothroyd, A. P. Crawley, and W. M. Stobbs, Phil. Mag. A 54 (1986) 663.

[64] P. W. Tasker and D. M. Duffy, Phil. Mag. A 47 (1983) L45.

[65] D. Wolf, Mater. Res. Soc. Symp. Proc. 24 (1984) 47.

[66] M. Mills, private communication .

[67] K. L. Merkle, Colloque de Phys. 51 (1990) C1-251.

[68] R. C. Pond and D. A. Smith, Can. Metall. Quarterly 13 (1974) 39.

[69] K. L. Merkle, Scripta Met. 23 (1989) 1487.

[70] V. Vitek, A. P. Sutton, G. J. Wang, and D. Schwartz, Scripta Met. 17 (1983) 183.

[71] L. M. Clarebrough and C. T. Forwood, Phys. Stat. Sol. A 60 (1980) 51.

[72] C. T. Forwood and L. M. Clarebrough, Acta Met. 32 (1984) 757.

[73] W. Krakow and D. A. Smith, in Grain Boundary Structure and Related Phenomena, Ed. Y. Ishida, Trans. Jap. Inst. Met. **27**, (1986) p. 277.

[74] P. J. Goodhew, T. Y. Tan, and R. W. Balluffi, Acta Met. 26 (1978) 557.

[75] H. Gleiter, Mater. Sci. Eng. 52 (1982) 91.

[76] D. Wolf, (1990) submitted to J. Appl. Phys.

[77] N. F. Mott, Proc. Phys. Soc. 60 (1948) 391.

[78] A. P. Sutton, Phase Transitions 16/17 (1989) 563.

[79] C. B. Carter, Acta Met. 36 (1988) 2753.

[80] T. Hasegawa, K. Kobayashi, N. Ikarashi, K. Takayanagi, and K. Yagi, Jap. Journ. Appl. Phys. 25 (1986) 366.

Figure Captions

Fig. 1. Macroscopic characterization of grain boundaries. (a) A bicrystal is characterized by the misorientation axis $\mathbf{t}$ (2 DOFs) and the misorientation angle θ (1DOF). The boundary plane is defined by its normal $\mathbf{n}$. Note that $\mathbf{n}\cdot\mathbf{t}=0$ for tilt GBs. (b) An alternate way of defining a grain boundary is given by specifying the crystallographic planes $(h_1k_1l_1)$ and $(h_2k_2l_2)$ that are joined at the interface (4 DOFs) and a twist angle ψ (1 DOF). Tilt GBs (or the ideal lattice are formed for $\psi=0°$ and $\psi=180°$.

Fig. 2. Two interpenetrating lattices in (a) produce the coincident site lattice (CSL indicated by circled atoms), $\Sigma=17$, $\theta=28.07°$. Two layers of atoms in the <001> projection of the fcc lattice are indicated by different size symbols. The arrows indicate the position of one set of the two different types of planes for symmetric tilt GBs. (b) A GB is generated from (a) by discarding white and black atoms on opposite sides of the interface (open arrows in (a) indicate the GB plane). The structural repeat unit of this asymmetric (100)(8,15,0) GB is given by twice the distance between CSL points along the (100) plane.

Fig. 3. (a) Two cube-on-cube oriented fcc lattices with incommensurate lattice parameters superimposed. Regions of good and poor atomic match can be readily recognized. (b) Incoherent interface is produced by joining the rigid model crystals. When the atoms are allowed to relax, a two-dimensional network of misfit dislocations can be formed.

Fig. 4. The interface between Cu and NiO, observed at a Cu precipitate in NiO produced by internal reduction, is formed on (111) planes. In this HREM image, taken

along <1$\bar{1}$0>, it is seen that despite of the large misfit (14%), misfit localization has taken place (black atomic columns).

Fig. 5. NiO precipitates formed in Pd by internal oxidation (white atomic columns). (a) In the cube-on-cube orientation. (b) In the twin related orientation. Both precipitates show complex interface contrast due to three-dimensional relaxations near the interface.

Fig. 6. Ag/NiO interface shows one misfit dislocation (indicated by arrow) which terminates at several atomic distances from the interface. This stand-off effect allows the interface between Ag and NiO to be coherent right at the interface.

Fig. 7. Misfit dislocations in the (111) Ni/Ag interface (white atomic columns). (a) Somewhat delocalized misfit dislocation. Black dots indicate Burgers circuit. (b) Ni/Ag interface and (c) corresponding image simulation, based on the relaxed atomic model obtained by EAM calculation [8]. Foil thickness t=7 nm, objective lens defocus Δf=-70 nm. White dots represent the metal columns in both Ag and Ni crystals.

Fig. 8. <1$\bar{1}$0> tilt bicrystal viewed along the tilt axis. The small island grain of Au shows pronounced symmetric and asymmetric facets. Misorientation θ=50°, Σ=11.

Fig. 9. Σ=5, (210) symmetric tilt GB in NiO. (a) The HREM image along the <001> tilt axis clearly does not have mirror symmetry. (b) Image simulation, based on (0 K) lattice statics calculations [44]. It can be easily seen that the experimentally observed structure has a much denser arrangement of atomic columns than the theoretical structure.

Fig. 10. False color images from image simulations of the (310) symmetric <001> tilt GB in NiO, based (a) on fully dense columns and (b) on introducing 25 % vacancies in the columns bordering the GB core. Thickness t=4 nm, defocus Δf=40 nm.

Fig. 11. Symmetric (310) , Σ=5 GB in NiO. (a) The HREM image (black atomic columns) clearly shows two different core structures for this GB with the same macroscopic GB parameters. The two facets are separated by a small step. Positioning of the interface at a different plane is equivalent to a rigid-body shift parallel to the GB, as schematically shown in (b) for a CSL boundary. The left hand side of fig. 11b shows the CSL, while the corresponding GBs for different planes (dashed lines) on the right have different rigid-body shifts parallel to the GB plane (compare relative positions of triangles). Note that for real crystals with a rigid-body translation, the additional shift due to the change in plane is the same as for the CSL model, and leads to a different core structure whenever the step is not a multiple of the interplanar spacing of the CSL.

Fig. 12. HREM image (white atomic columns) of $<1\bar{1}0>$ tilt bicrystal in Au, viewed along $<1\bar{1}0>$ tilt axis. Misorientation $\theta = 39°$ (Σ=9). The GB changes its inclination from the (114)(114) GB on the left to the dissociated (111)(115), and to the (11,11,1)(111) on the right.

Fig. 13. Faceted $<1\bar{1}0>$ tilt micrograin at bottom ($\psi = 50°$, Σ=11) shows four facets, ranging from the (113)(113) at the top of the figure, over (225)(441) and (557)(771) to the (332)(332) GB. Note that the (113)(113) is fully coherent, while both asymmetric GBs show extended strain contrasts in the top grain, with little evidence for elastic distortions in the bottom grain.

Fig. 14. HREM image of the (443) symmetric tilt GB, Σ=41, θ=55°. Note the misfit localization and the strong tendency to maintain coherence between dense-packed planes. The compressed image (bottom), clearly shows the correlations between atomic positions in the near-core region.

Fig. 15. <001>, Σ=13, tilt GBs in NiO (black atomic columns). (a) (510) GB showing coherence between (010) planes crossing the interface. (b) GB with several microfacets also shows coherence between low-index planes crossing the interface.

Fig. 16. Asymmetric (111)(001), $<1\bar{1}0>$ tilt GB in Au. The GB shows misfit localization in the form of misfit-dislocation-like defects. The centers of misfit are arranged in a periodic fashion, but the GB is in fact quasiperiodic, since the atomic distances along the GB are incommensurate. The compressed image at the bottom of the figure indicates that the misfit localization is accompanied by slight elastic distortions in the surrounding lattice.

Fig. 17. Asymmetric (210)(100) GB in NiO (black atomic columns). Well-structured, interfaces along low index, incommensurate planes are frequently found in NiO.

Fig. 18. Symmetric (338)(338) GB in Au. Tilt axis $<1\bar{1}0>$, θ=55°, Σ=41. The GB shows strong coherence between (111) planes crossing the interface. The misfit is accommodated by stacking faults which extend to both sides of the interface, where they are terminated by partial dislocations. The stacking faults are arranged in quasiperiodic fashion (see text).

Table 1: Heterophase Boundaries

Interface	Misfit $\|\eta\|$	Preparation
NiO/Cu	0.14	Internal reduction
NiO/Pd	0.07	Internal oxidation
NiO/Ag	0.02	Thin-film technique
CdO/Pd	0.19	Internal oxidation
CdO/Ag	0.14	Internal oxidation
Ag/Ni	0.15	Thin-film technique
Au/Ni	0.15	Thin film technique

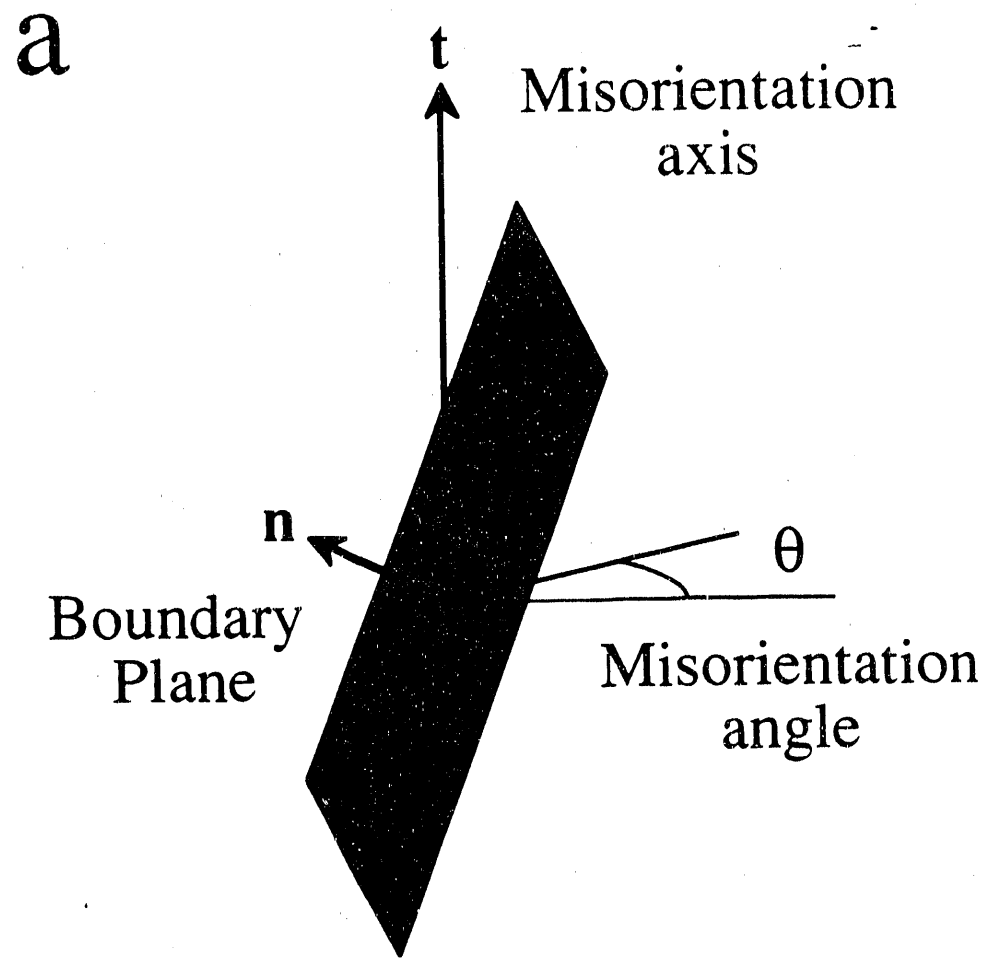
a
t
Misorientation
axis
n
θ
Boundary
Plane
Misorientation
angle

Fig. 1a

b

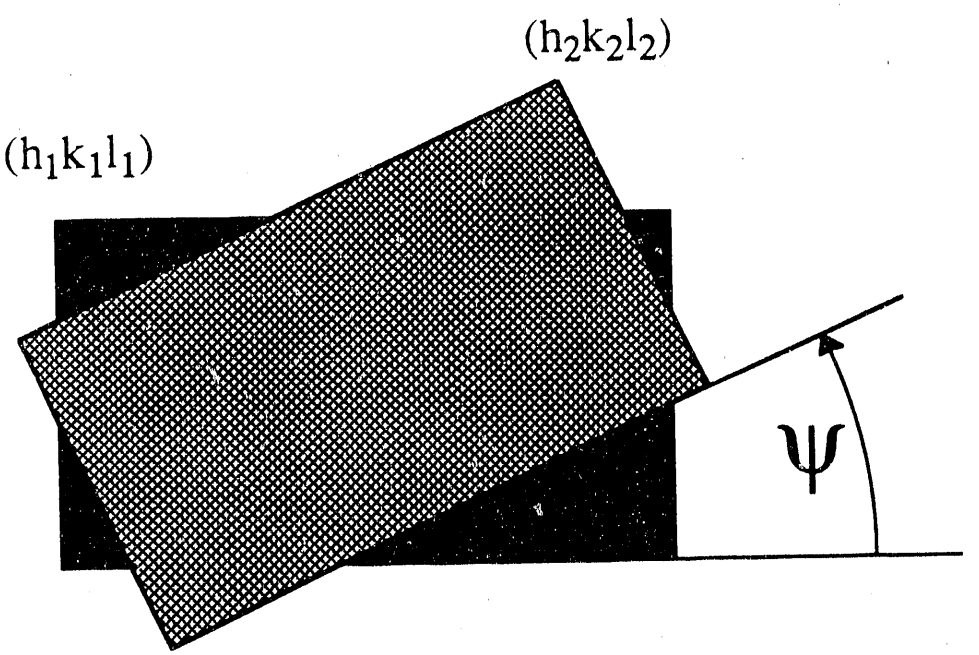

Fig. 1b

a

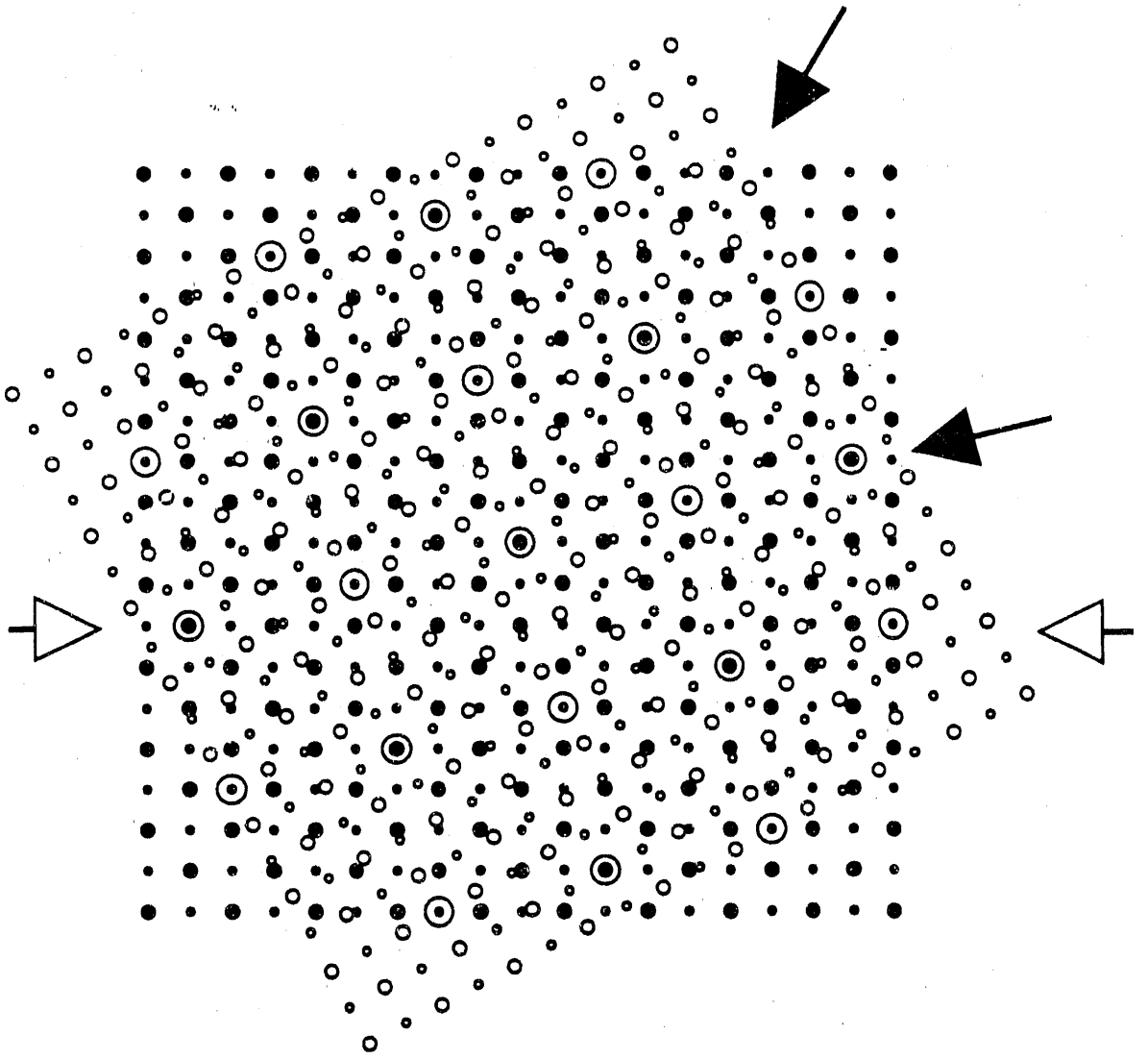

b

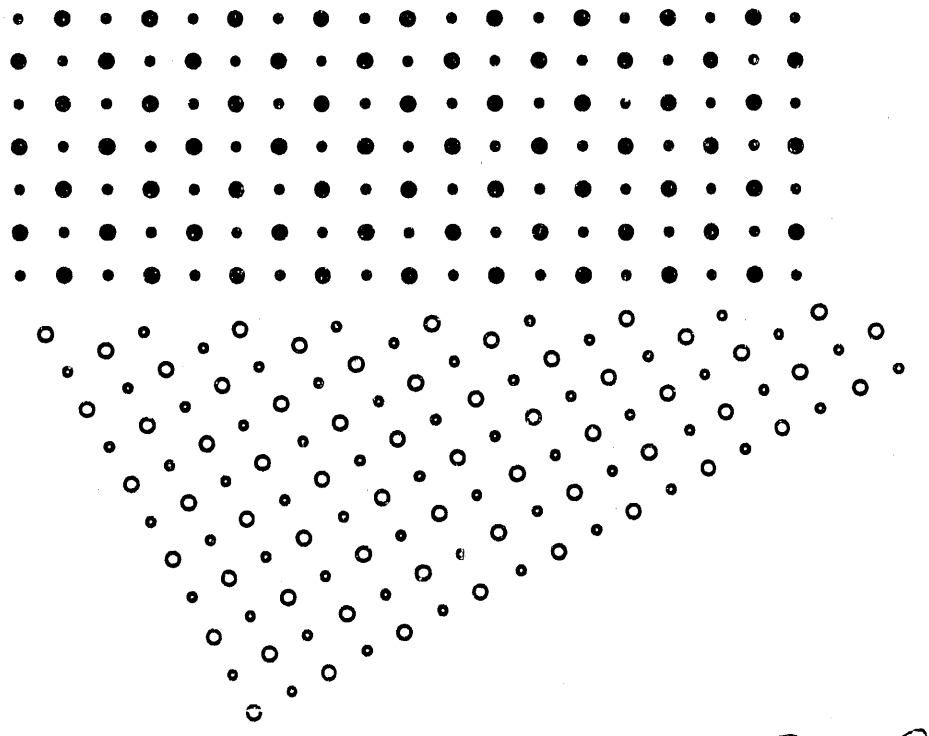

Fig. 2

a

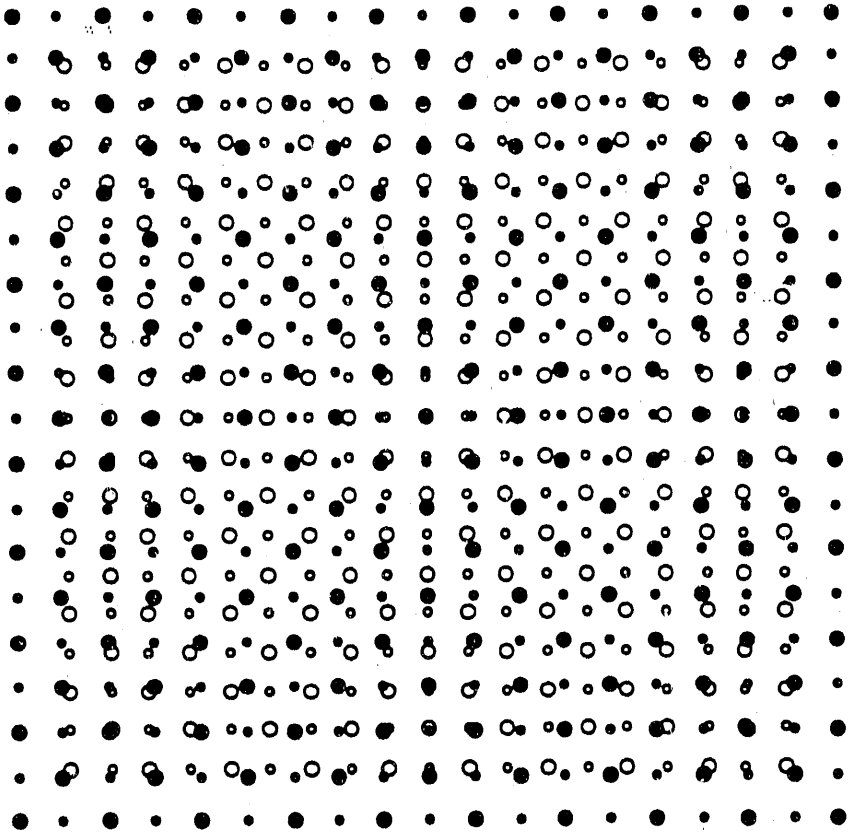

b

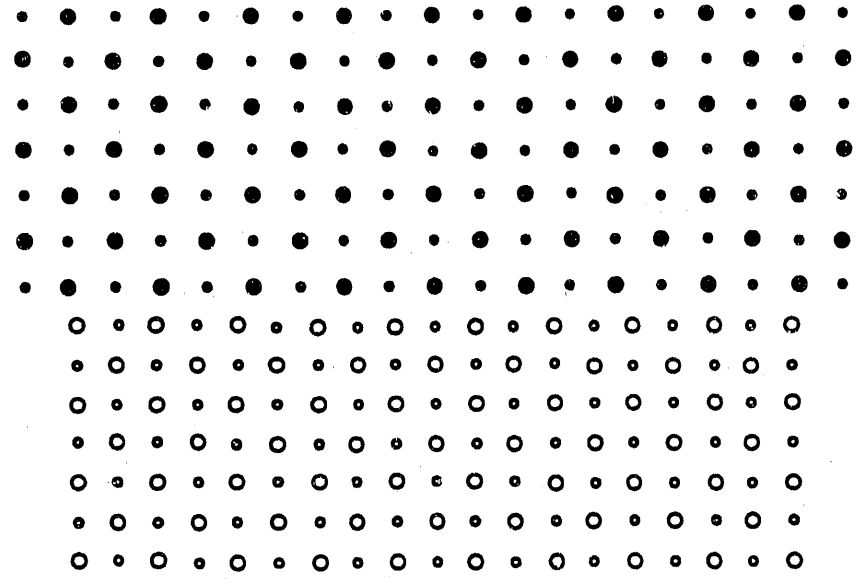

Fig. 3

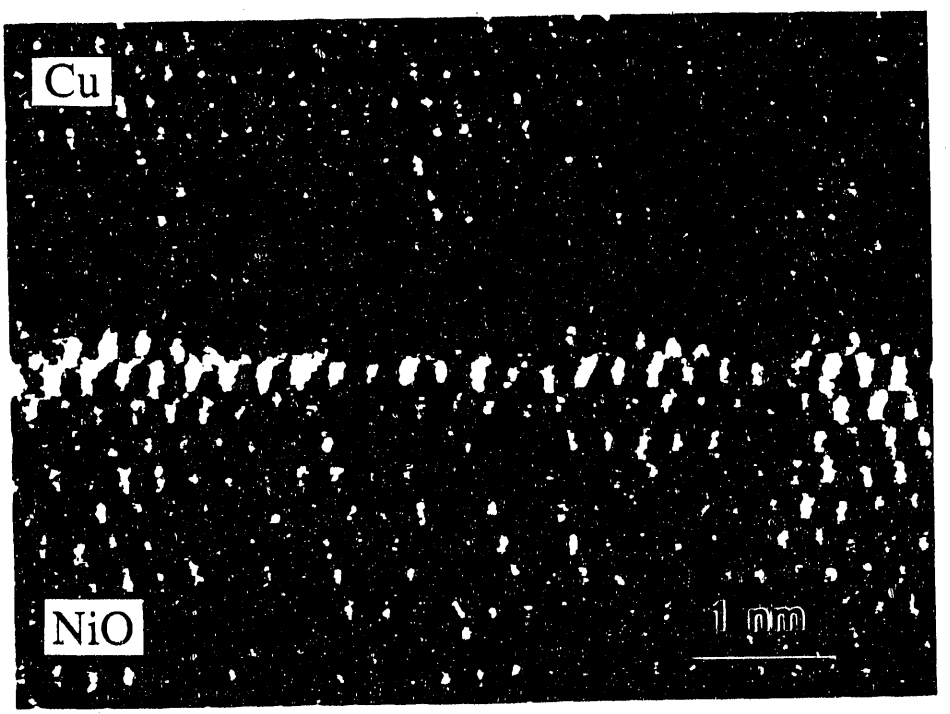

Fig. 4

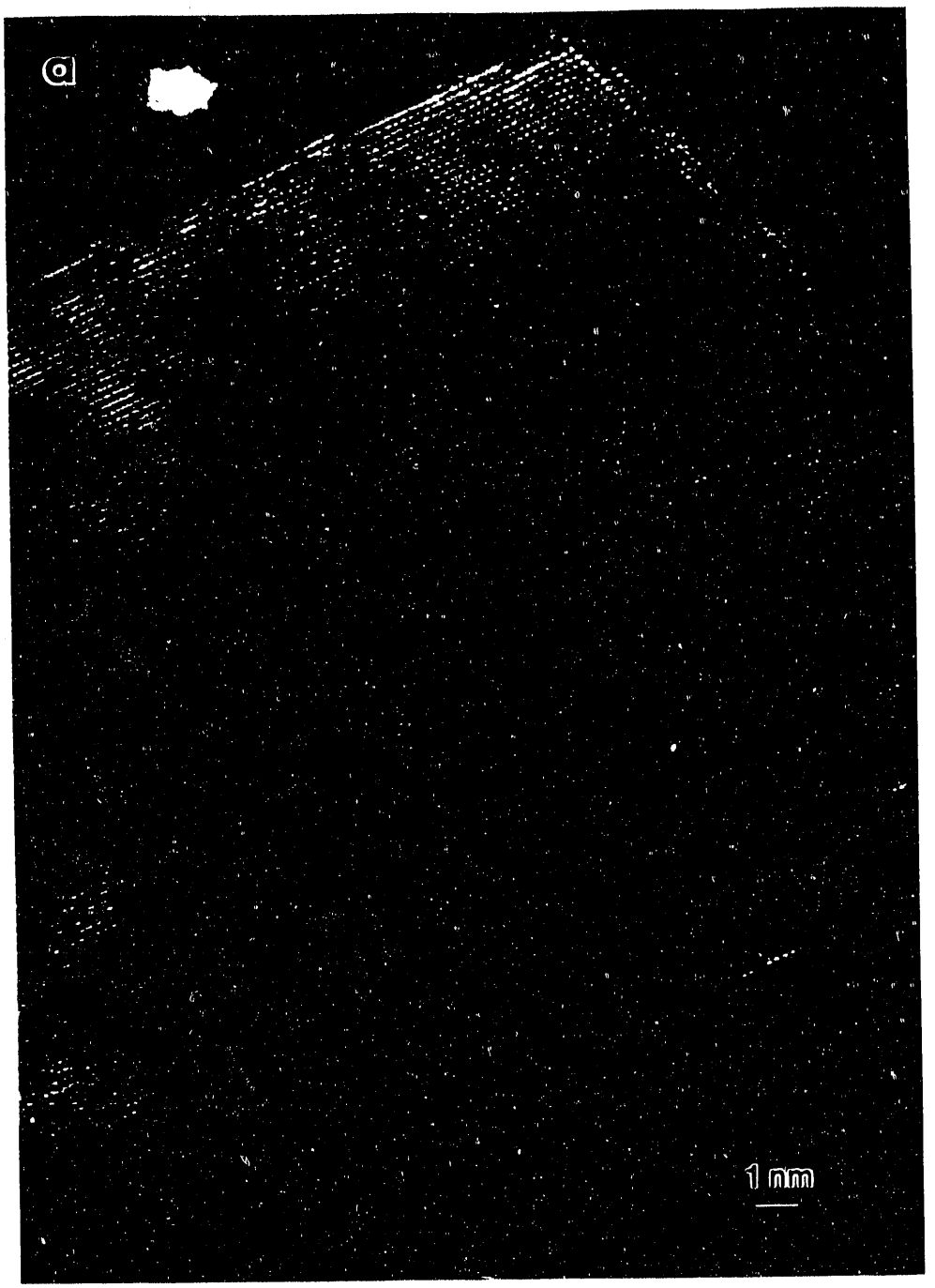

Fig. 5a

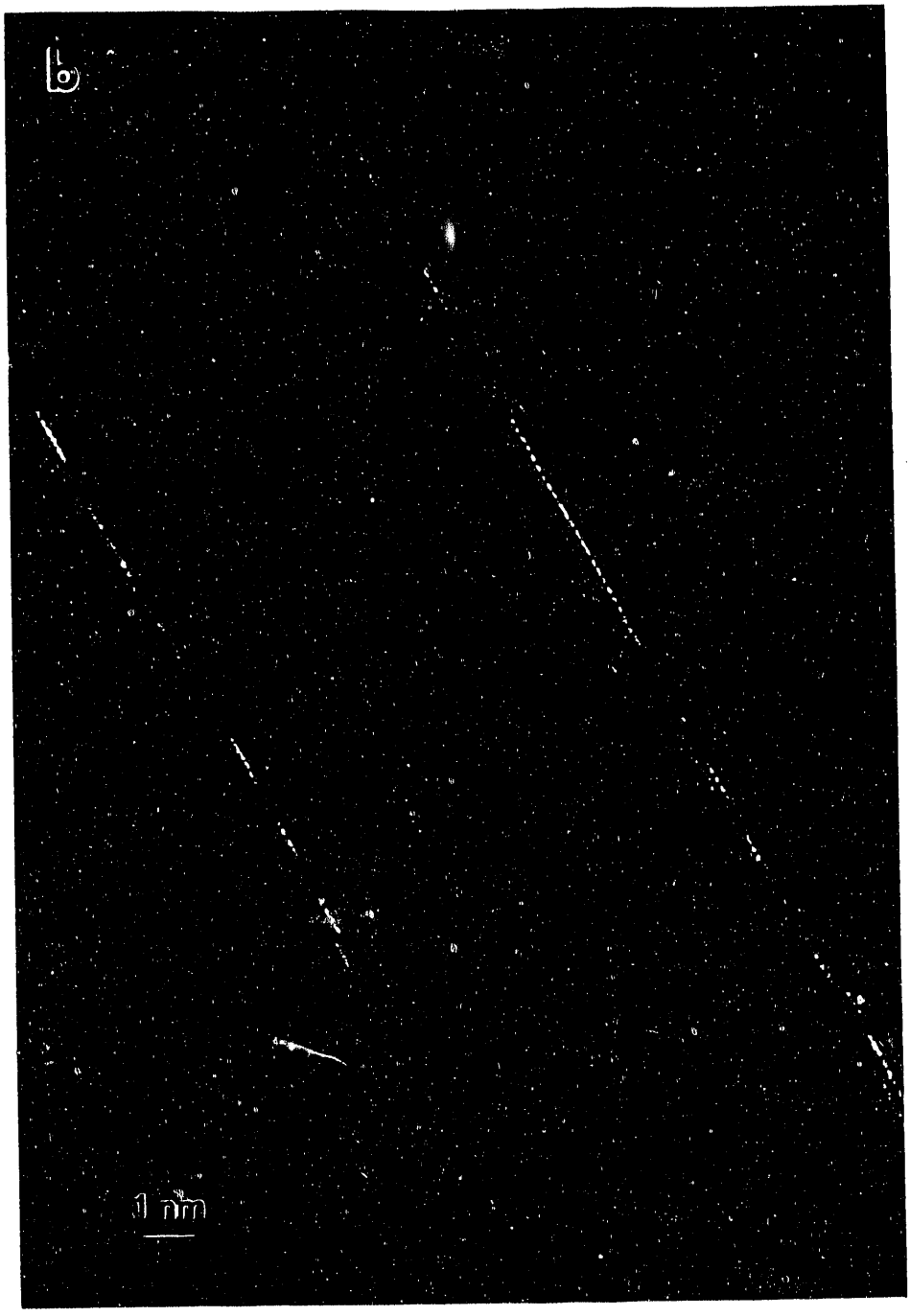

Fig. 5b

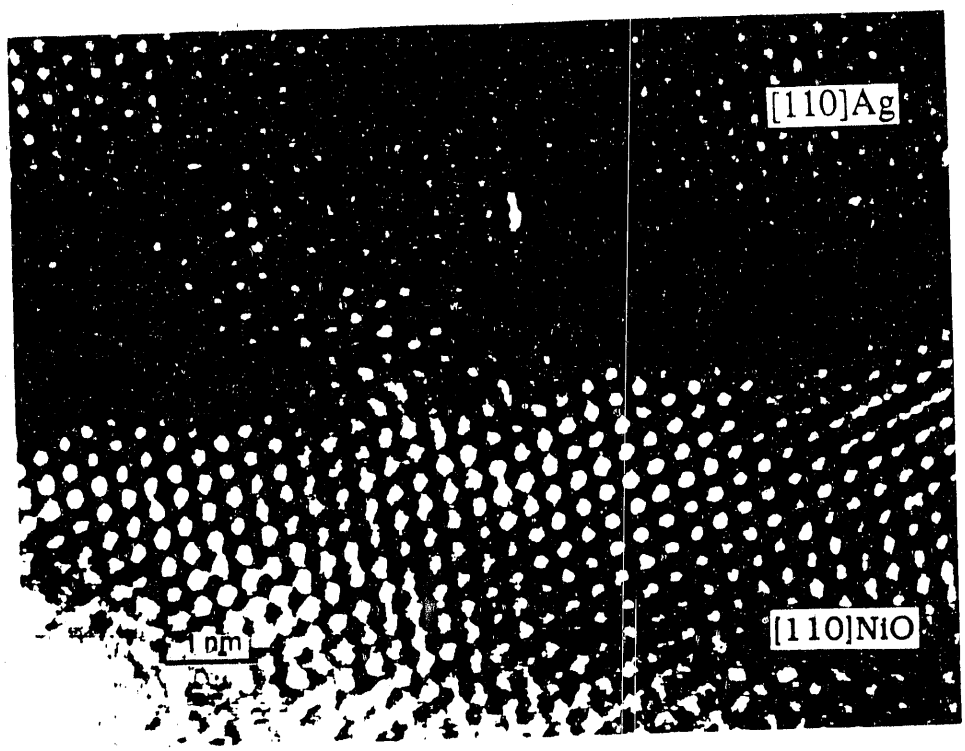

Fig. 6

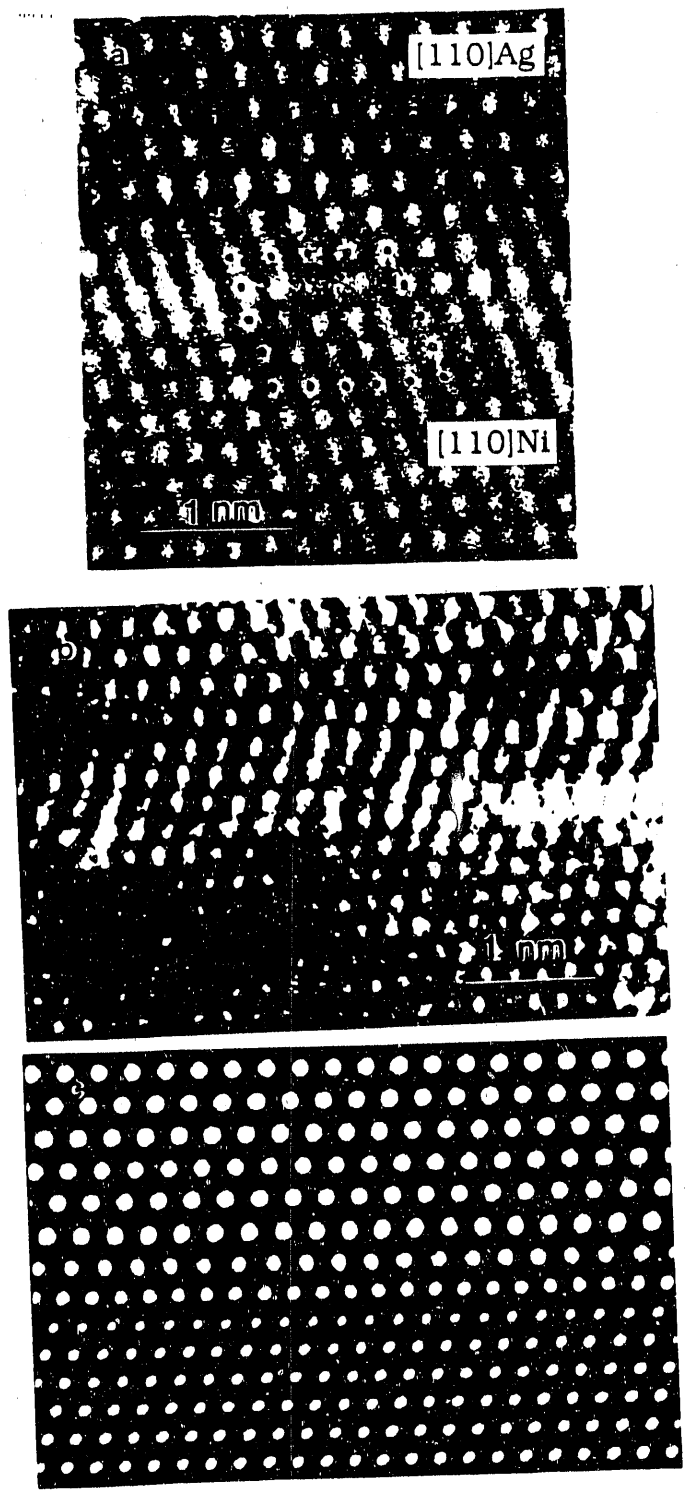

Fig. 7

crystals. When the atoms are allowed to relax, a two-dimensional network of misfit dislocations can be formed.

Fig. 4. The interface between Cu and NiO, observed at a Cu precipitate in NiO produced by internal reduction, is formed on (111) planes. In this HREM image, taken

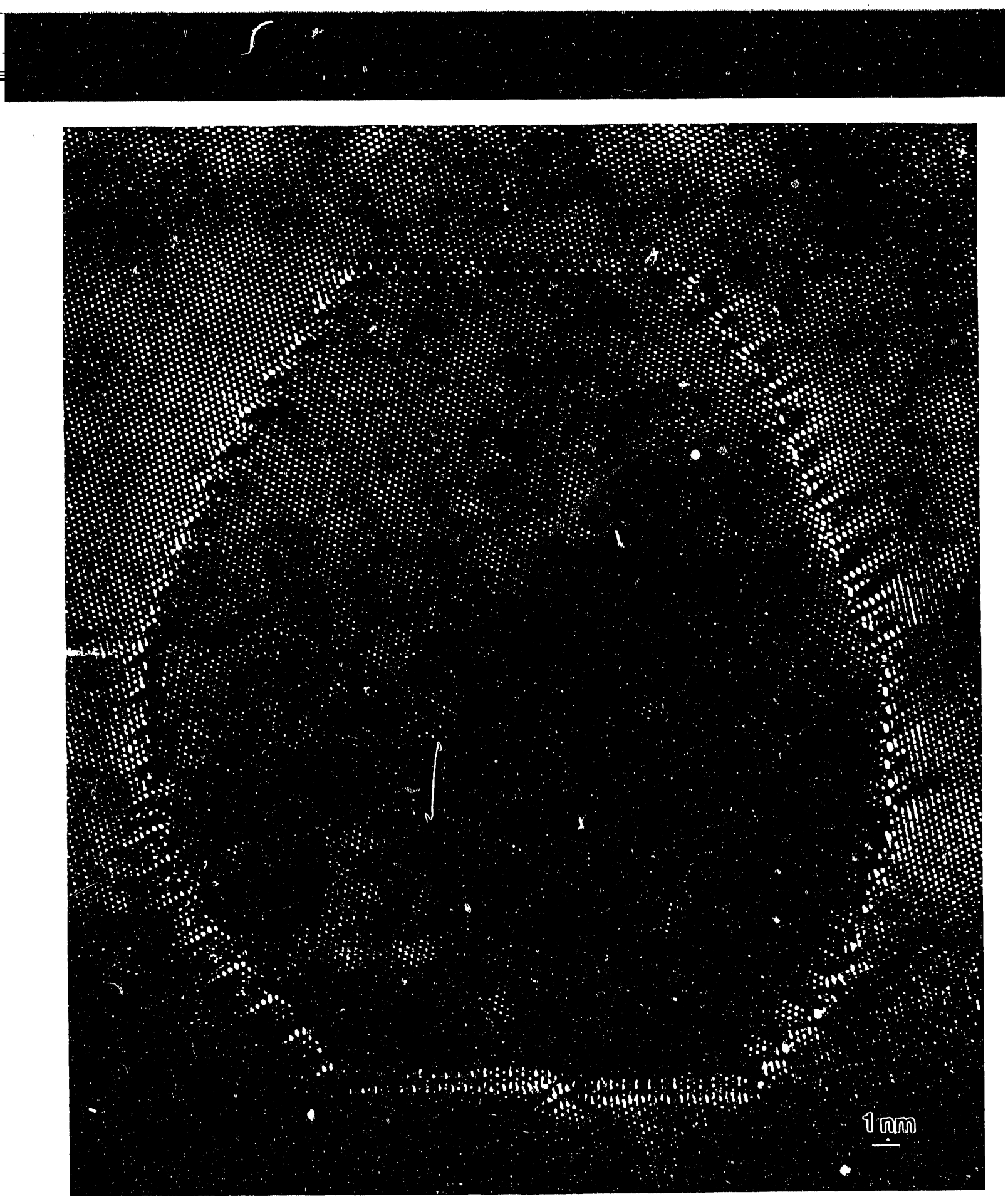

Fig. 5

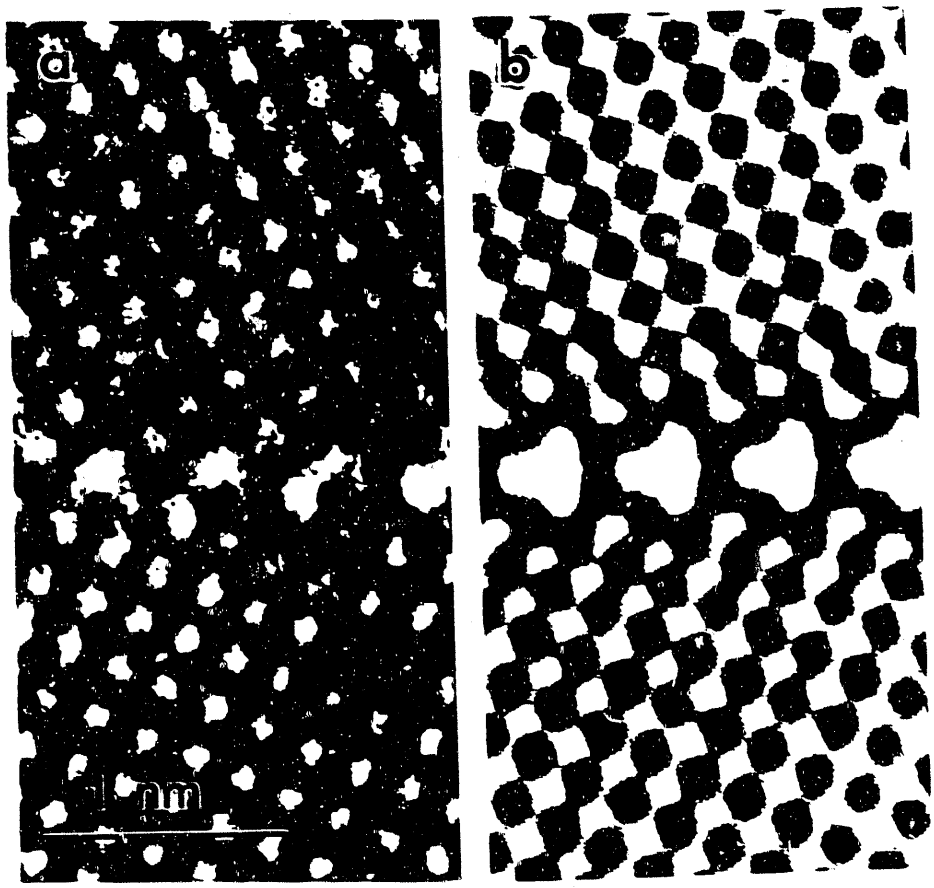

Fig. 9

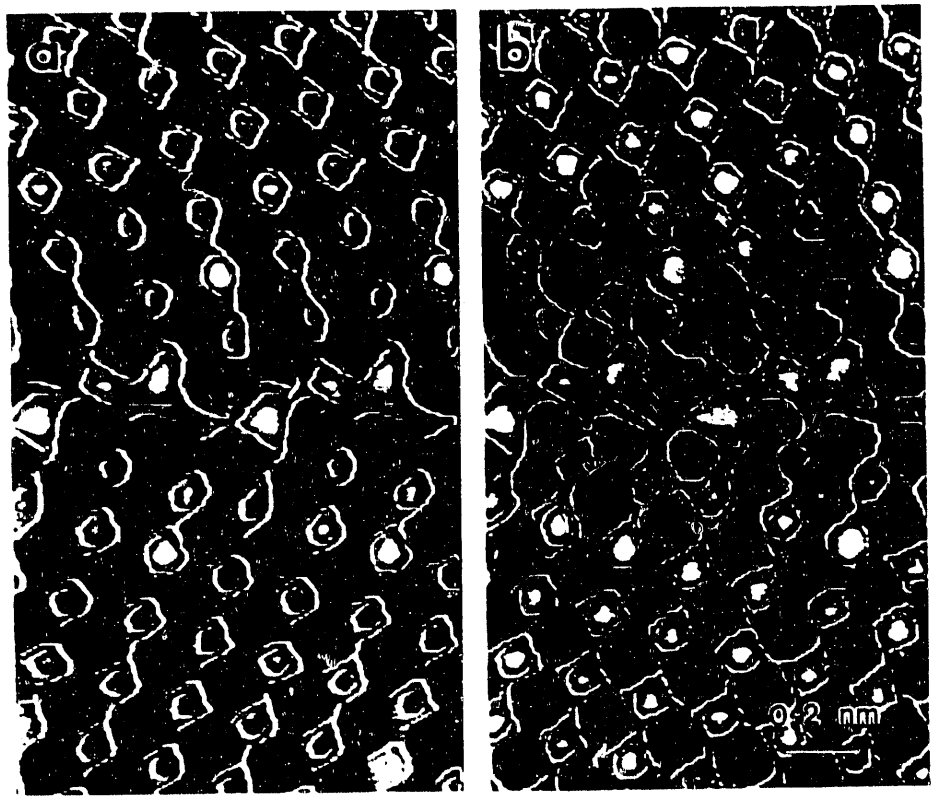

Fig. 10

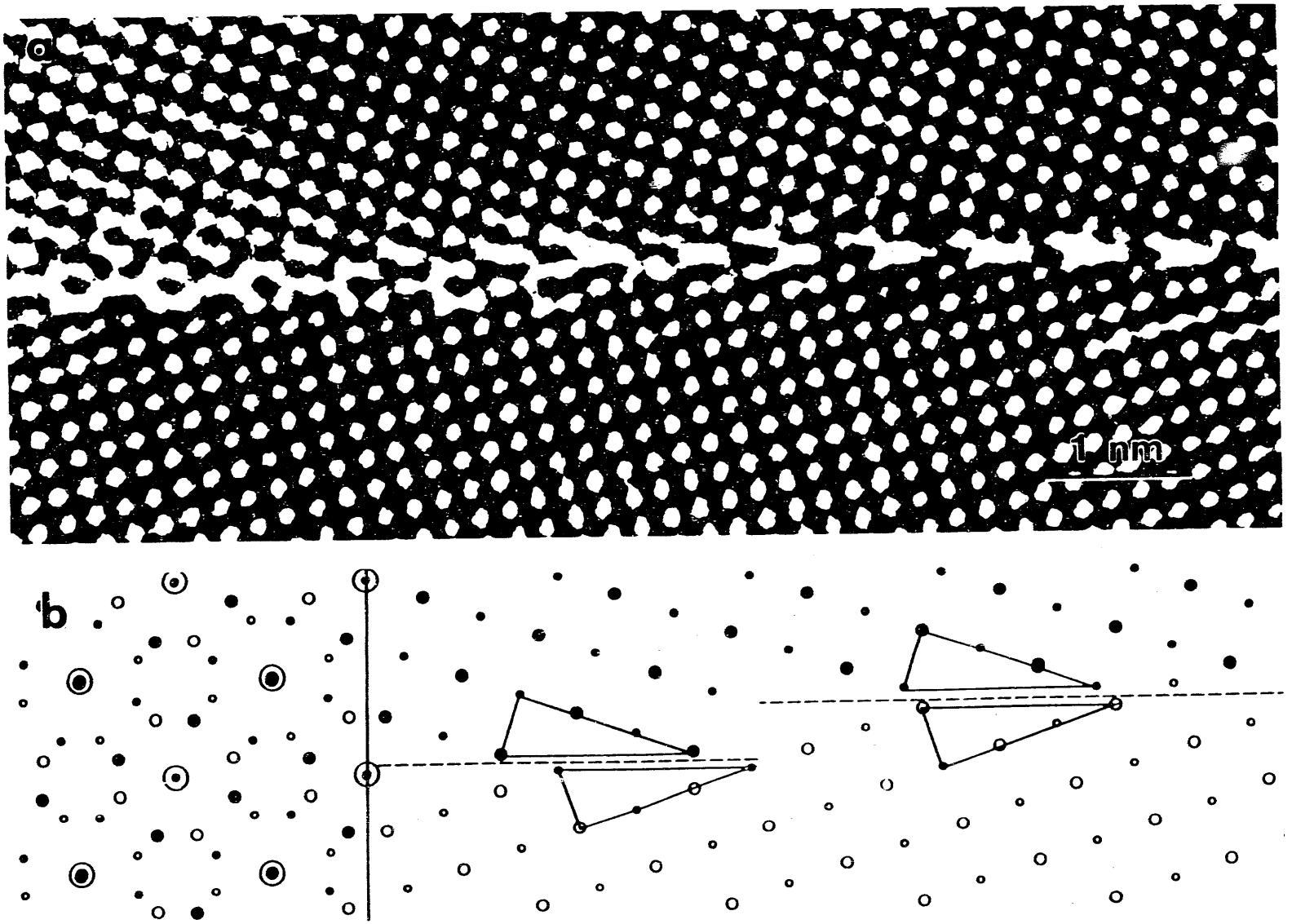
a
1 nm
b

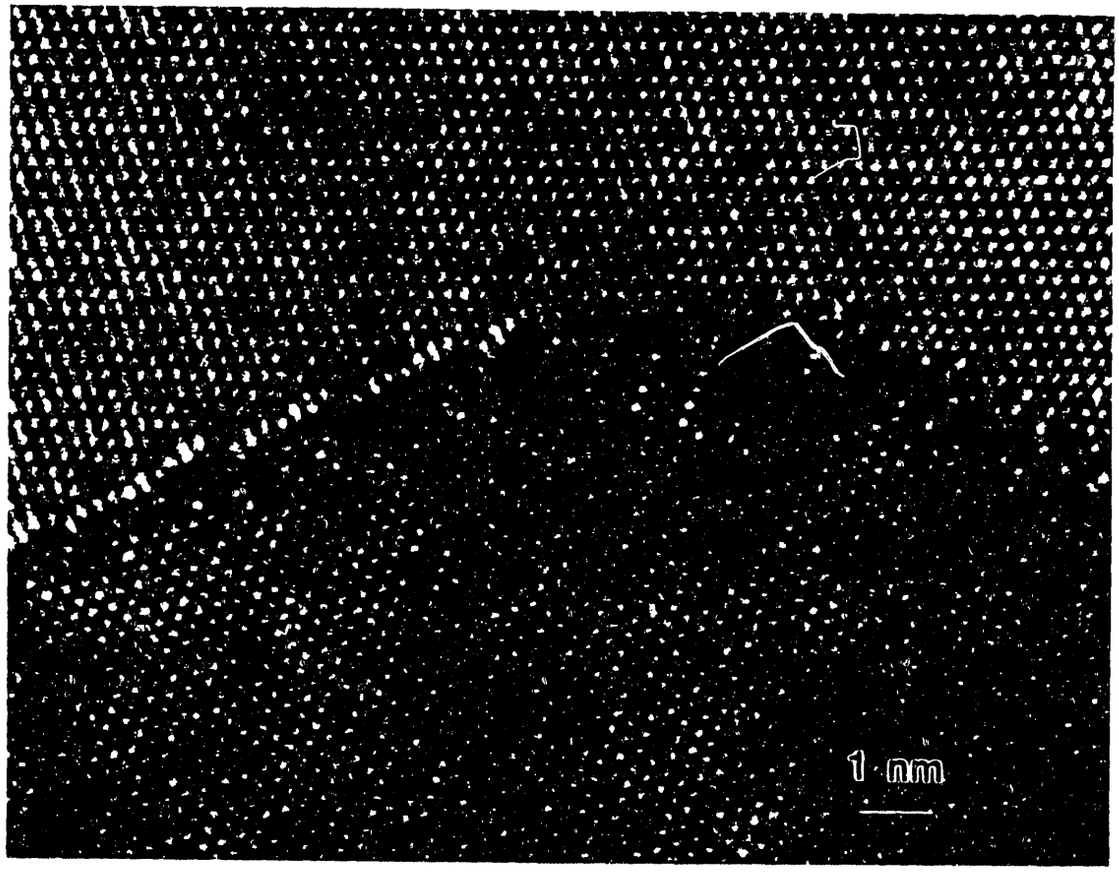

Fig. 12

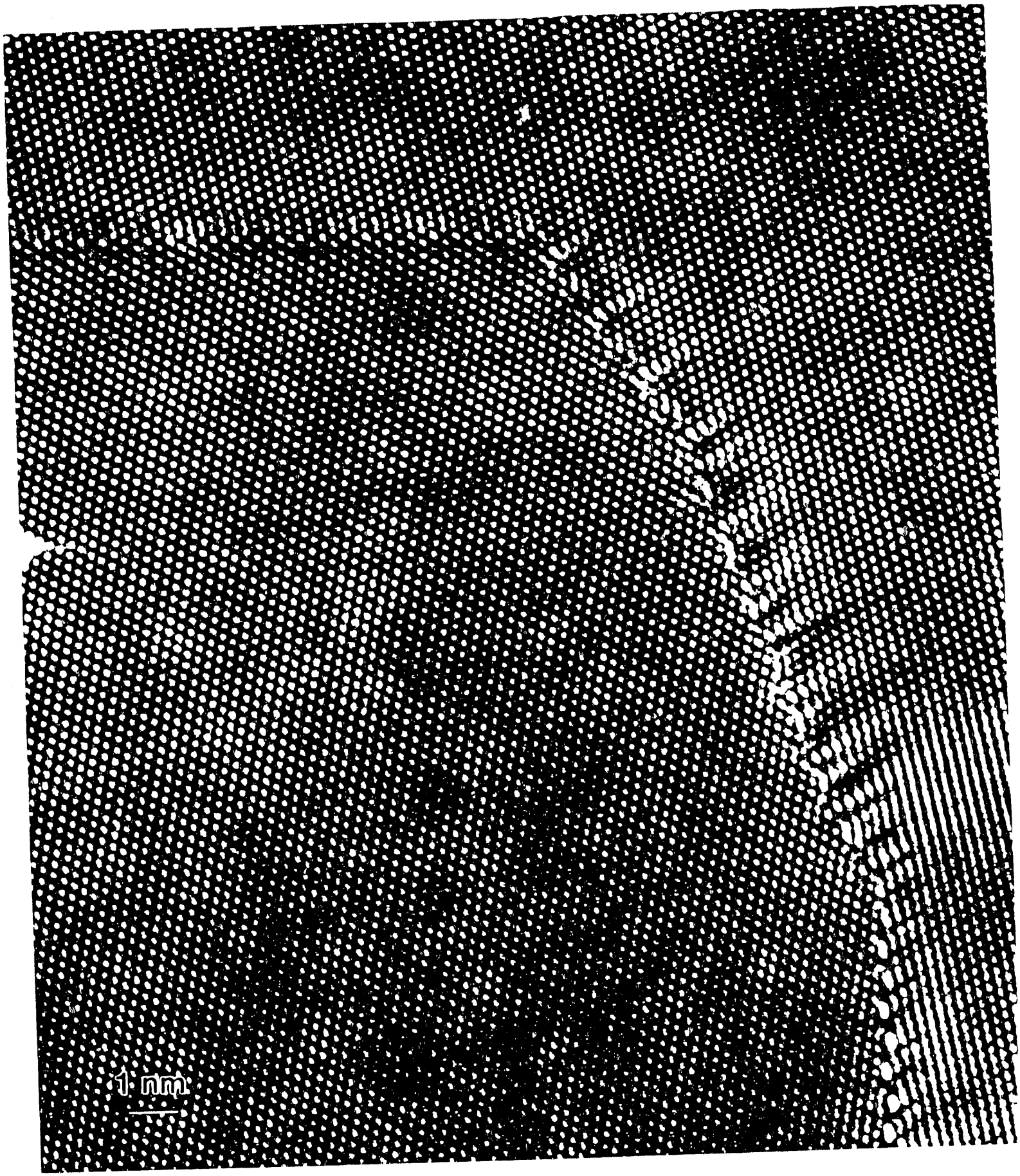
1 nm

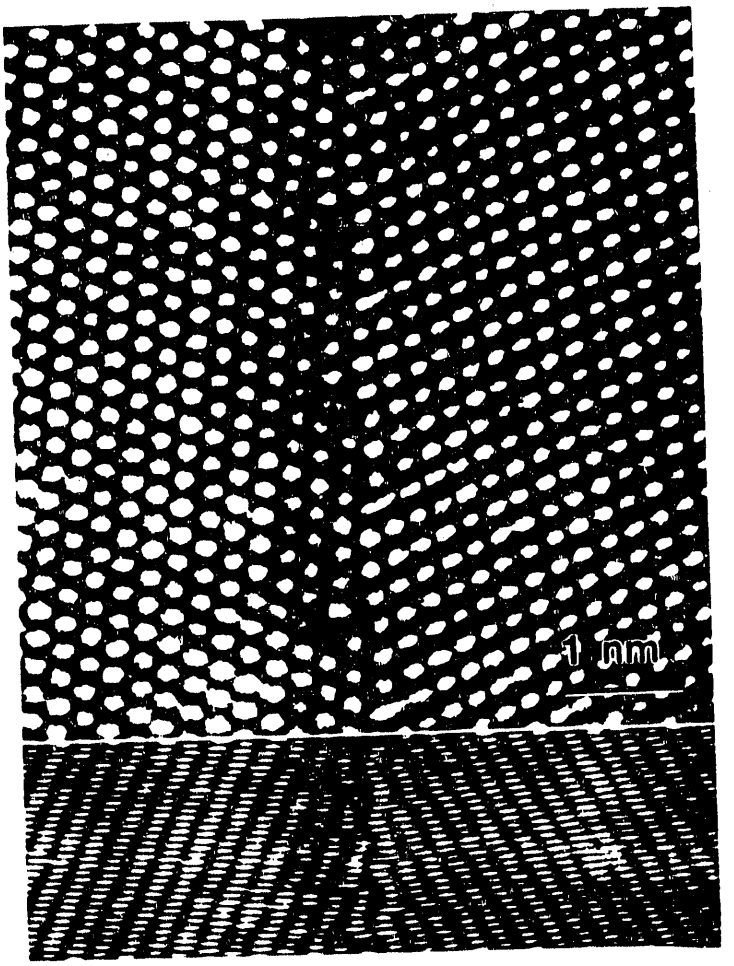

Fig. 14

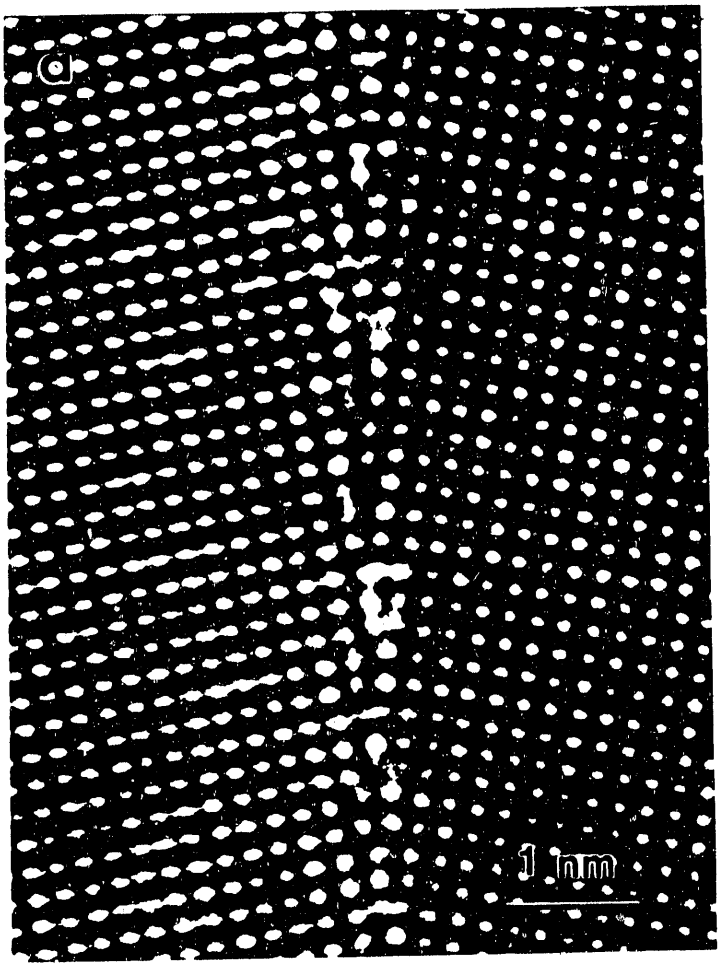

Fig. 15a

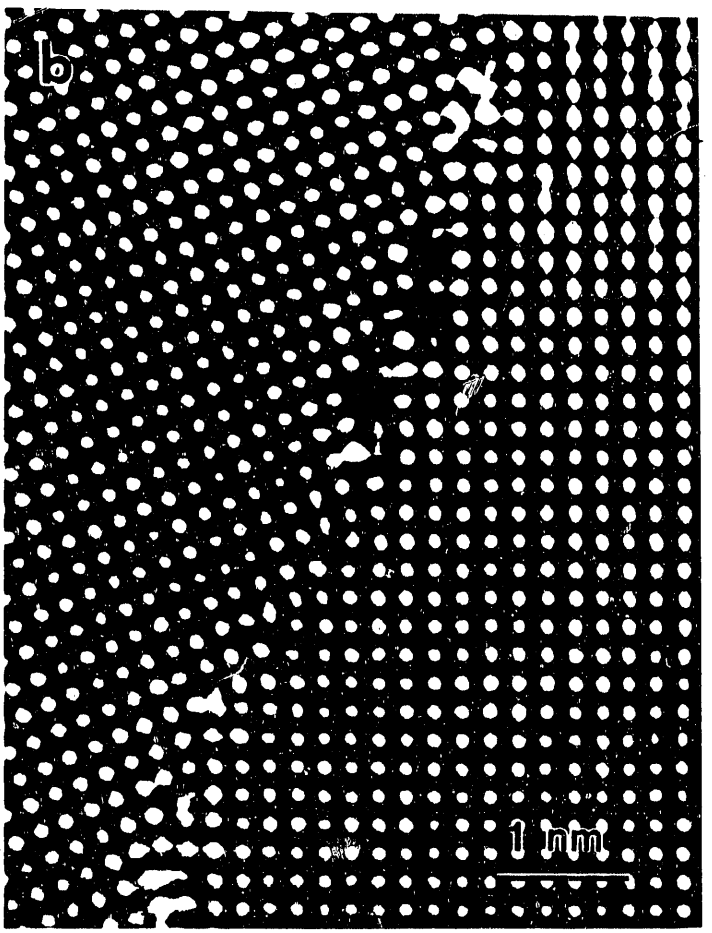

Fig. 15b

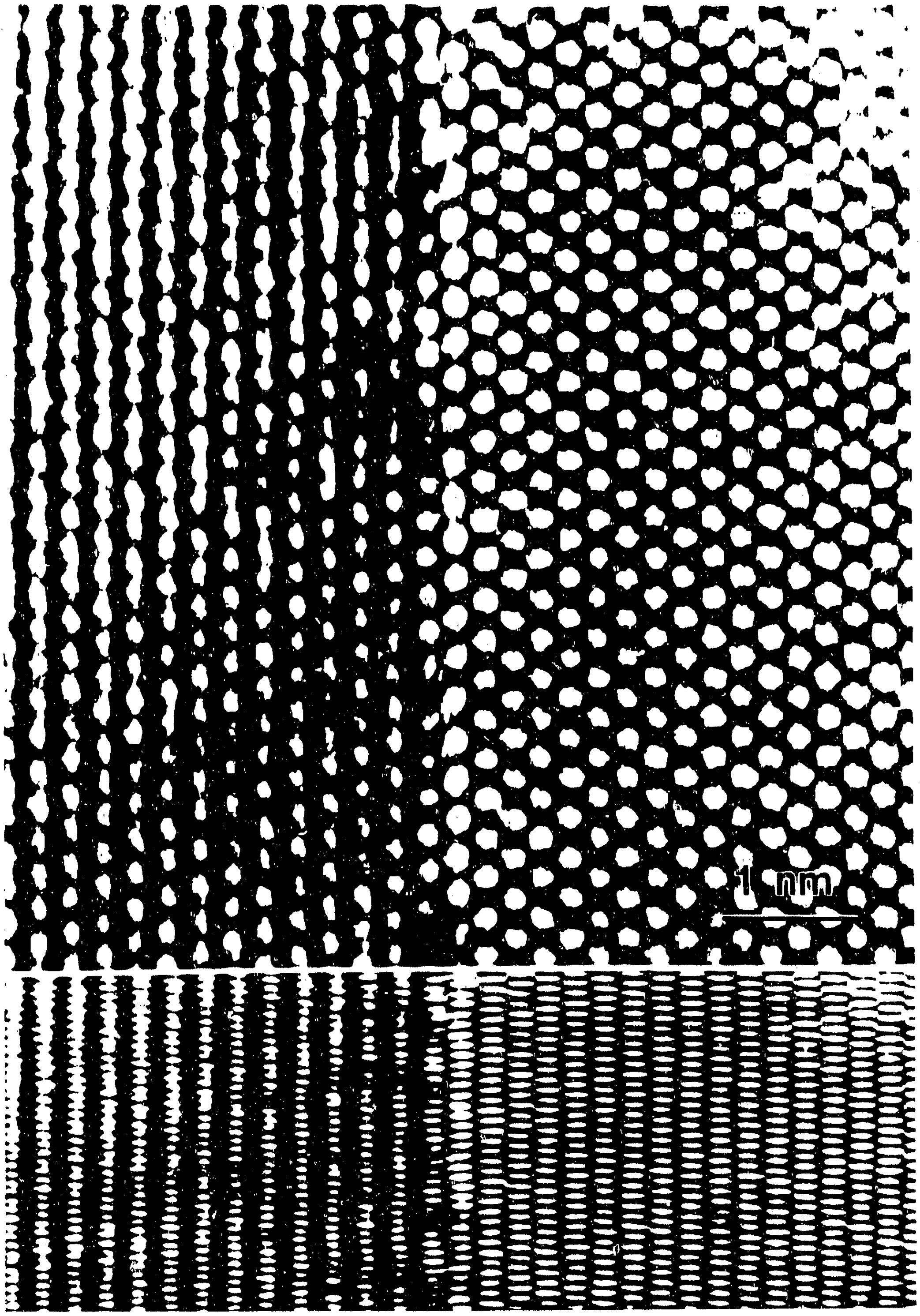

Fig. 6

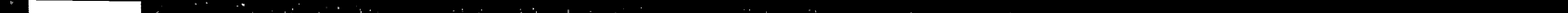
1 nm

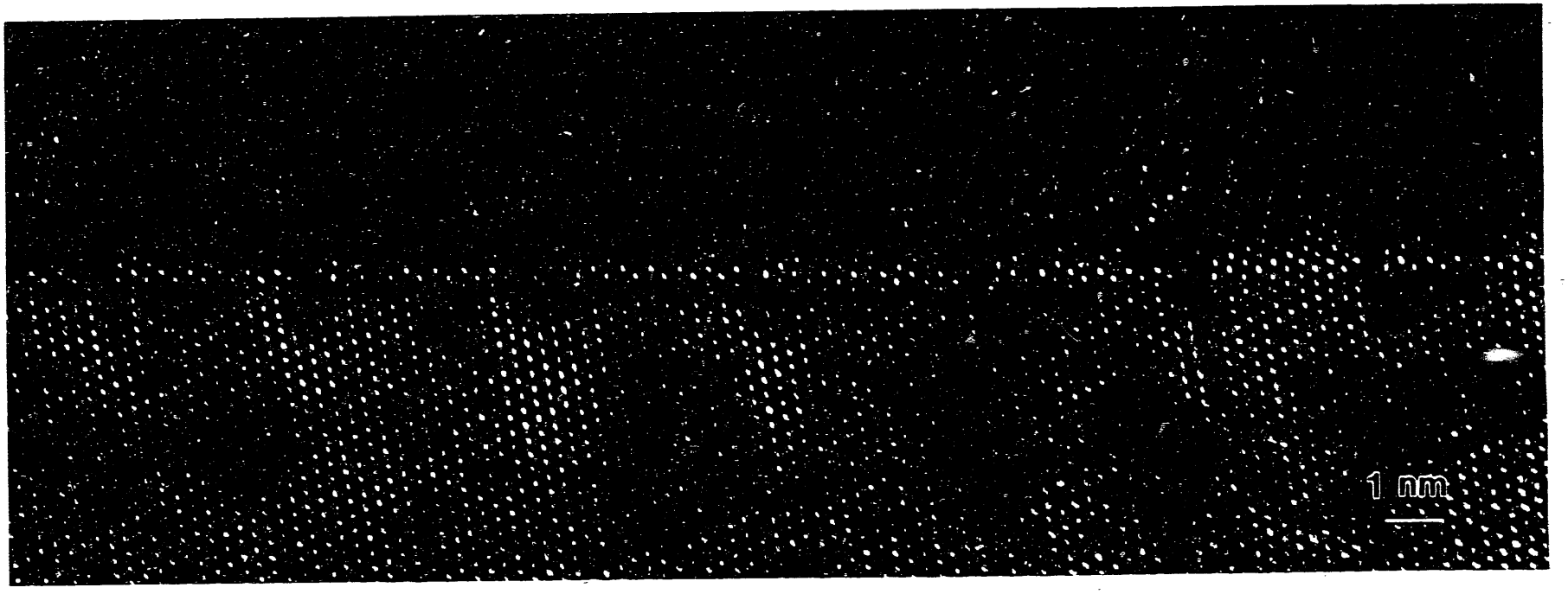

Fig. 18

END

DATE FILMED

12/20/90